SKI Report 2004:51

Research

Investigation of the Potential for In-Vessel Melt Retention in the Lower Head of a BWR by Cooling through the Control Rod Guide Tubes

APRI 4, Stage 2 Report

B.R. Sehgal
A. Jasiulevicius
M. Konovalikhin

January 2004

ISSN 1104–1374
ISRN SKI-R-04/51-SE

SKI

The APRI 4 (Accident Phenomena of Risk Importance) research project is accomplished by:

- Swedish Nuclear Power Inspectorate
- Ringhals AB
- OKG Aktiebolag
- Forsmarks Kraftgrupp AB
- Barsebäck Kraft AB
- Teollisuuden Voima Oy (TVO)

and supervised by the Project Board, consisting of:

OKG Aktiebolag	Mauritz Gärdinge, chairman
Swedish Nuclear Power Inspectorate	Oddbjörn Sandervåg
Swedish Nuclear Power Inspectorate	Ninos Garis
Ringhals AB	Anders Henoch
Forsmarks Kraftgrupp AB	Ingvar Berglund
Barsebäcks Kraft AB	Erik Larsen
TVO	Heikki Sjövall
Safetech Engineering	Stig Rolandsson (project leader)

SKI Report 2004:51

Research

Investigation of the Potential for In-Vessel Melt Retention in the Lower Head of a BWR by Cooling through the Control Rod Guide Tubes

APRI 4, Stage 2 Report

B.R. Sehgal
A. Jasiulevicius
M. Konovalikhin

January 2004

SKI Project Number 00046

CONTENTS

EXECUTIVE SUMMARY

This report describes the experiments performed at the Division of Nuclear Power Safety of the Royal Institute of Technology (KTH) investigating the coolability potential offered by the Control Rod Guide Tubes (CRGTs), which are present in large numbers in the lower head of a BWR and there is a water flow circuit in each one of them. This investigation is related to the overall goal of retaining the core melt in the lower head of a BWR during a postulated severe accident, through accident management procedures, or strategy.

The experiments were performed in two facilities, i.e. POMECO (POrous MEdium COolability) and COMECO (COre MElt COolability), respectively, for investigating the coolability when the core material is in the form of a particulate debris bed and when it is in the form of a melt. The POMECO facility employed a sand bed heated electrically to heating levels of up to 1 MW/m^3 and experiments performed in that facility obtained the enhancement in the dryout heat flux and in the quench velocity due to presence of a CRGT, with, and without, water flow in it. The COMECO facility employed a simulant material melt pool heated electrically to power levels of $\approx$ 1.3 MW/m^3 and the experiments in it also determined the enhancement in the heat removal from the melt pool that could be obtained by the presence of a CRGT, with, or without water flow in it . In each of the experiments in these facilities, the scaling employed was of a unit cell of core material around a prototypic geometry CRGT with the prototypic decay heat input.

The experimental results showed that a CRGT is able to offer a substantial additional potential for coolability of particulate and melt material in the lower head of a BWR. Analysis of the data obtained in the set of experiments performed lead to the following results for the heat flux through the CRGT:

- for a water filled particulate debris bed: ~ 40 kW/m^2;
- for a day hot particulate debris bed: ~ 150 kW/m^2;
- for a melt pool with a crust formed on the CRGT surface: ~350 kW/m^2.

It is recommended that further investigations, both experimental and model development, be conducted to (a) check reproducibility of data (b) employ different flow rates (c) employ different simulant materials and (d) develop a comprehensive model, in order to certify that the coolability that can be achieved with establishing a water flow in the CRGTs will be able to retain the melt in the lower head of a BWR. We believe it will be an extremely important accident management strategy for a Swedish BWR since it will obviate the consideration of the prime licensing issue of ex-vessel steam explosion induced containment failure associated with the present scheme of establishing a water pool in the lower drywell of all the Swedish BWRs.

INTRODUCTION AND BACKGROUND

The postulated severe accident scenario for a BWR, in general, results in the core melt transferring from the original core geometry to the lower head. The BWR vessel being larger than that of PWR, containing a forest of control rods and a larger quantity of water will provide the conditions for core melt to break up and form a debris bed. This heat generating debris bed could become dry if water supply to the vessel is not resumed and in time could melt and form a melt pool in the lower head. This melt pool would start natural circulation and in time, it is possible that the vessel would fail due to the thermal loading imposed.

It has been recognized by almost all of the reactor safety community that it would be wise to retain the core melt within the lower head. This recognition has resulted in the design of the next generation reactors: AP-600, AP-1000 and SWBR-1000 employing accident management strategies which will retain the melt within the lower head for the postulated severe accidents. The principal accident management strategy is to establish a water pool in the PWR cavity or BWR drywell, which should provide sufficient heat removal on the outside of the lower head to retain the melt within the vessel lower head.

The Swedish BWRs designed by the ASEA Co. have a lower drywell and the vessel is very high above the bottom of the lower drywell. The accident management strategy employed by the Swedish BWRs establishes a pool of water in the lower drywell of 7 to 11 meters depth. The water level, however, is much below the vessel lower head and cannot provide coolability potential towards retention of the core melt within the lower head.

All BWR designs contain a forest of control rod guide tubes in the lower head. These guide tubes support (a) the B_4C-steel cruciform control blades which traverse through the length of the core and (b) the fuel subassemblies. Thus, these guide tubes are quite massive and contain appreciable heat capacity. They also have an annulus region through which there is a steady supply of subcooled water at the operating pressure. The flow rate, however, is not large; e.g., in the TVO plant the flow rate/CRGT is 62.5 grams/sec. This water, however, has sufficient heat capacity and latent heat to remove the decay heat after several hours. This water supply was the saviour of the Brown's Ferry fire induced "almost nuclear accident".

The question then, is whether the cooling capacity inherent in the heat capacity and the water supply of the multitude of CRGTs can be employed to cool the particulate debris bed, and the melt pool that may be formed in the lower head of a BWR as a result of a severe accident. It is assumed that the CRGTs have a water supply available throughout the accident, so that they do not melt or collapse when the debris bed heats up and later on forms the melt pool.

This is the subject of the investigations described in the present report. The approach of the study is to perform well-scaled experiments with simulant materials employing heat transfer conditions representative of the prototypic accident. Thus the temperatures for dry particulate debris bed are above the minimum film boiling temperature and the binary oxide melt composition employed had sufficiently high

liquidus and solidus temperatures and it formed crust on the cool surfaces of the CRGT. The scaling strategy employed a unit cell concept per CRGT, i.e., the particulate debris material and the melt associated / CRGT. The CRGT dimensions were prototypic and so was the heat input to the debris or melt surrounding a CRGT. We believe the results obtained can be applied directly for prototypic accident evaluations.

1. OBJECTIVES

The objective of the experimental program, performed at the NPS/RIT (Nuclear Power Safety Division of the Royal Institute of Technology) was to determine the capability for cooling of binary oxide melt and debris, deposited in the lower head of a BWR (Boiling Water Reactor) offered by the internal structures in the lower head. The debris bed in the BWR's could be formed as a consequence of a severe accident in this reactor type. In the LWR (Light Water Reactor) severe accident scenario, particulate debris beds are formed when corium melt comes in contact with water and a melt pool can form when the particulate debris bed re-melts if it is not cooled. Of particular importance is the coolability potential, that could be offered by the control rod guide tubes (CRGTs), which are located in the lower head of the reactor vessel, since:

(a) there is a large number of these tubes in the lower head;
(b) each of them offers a substantial additional heat transfer area;
(c) water is normally supplied to the guide tubes.

1.1 Geometry of the CRGT

We decided to employ the actual dimensions of the prototypic CRGT in the BWR-75 reactor, in order to develop a clear rationale for scaling in this experimental programme. The construction and dimensions of the lower part of the CRGT are presented in the Figure 1.1.

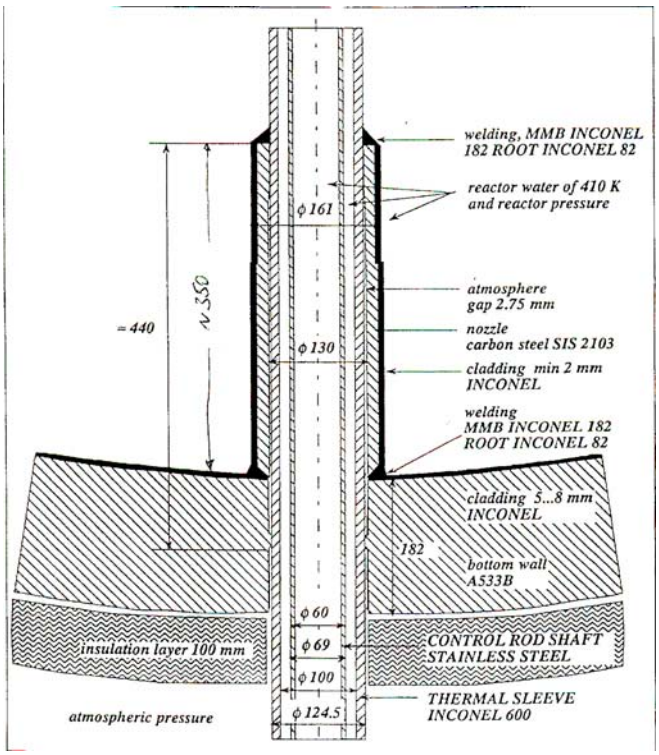

Figure 1.1 The bottom part of the Control Rod Guide Tube (CRGT) in the BWR-75 reactor

2. POMECO experiments

The POMECO (POrous MEdia COolability) facility was developed for experimental studies on coolability of heat generating particulate debris beds (Konovalihkin, et al, 1998, 2000). The test section was a stainless steel vessel. Cross section area of the vessel was 350×350 mm. Total height of the section was 1400 mm. Up to 370 mm of the sand bed could be formed to simulate the debris. The test section contained annular pipe of the same dimensions as CRGT in a typical BWR. The test section represented a unit cell with one CRGT for the BWR reactor lower head. Test section power was up to 1 MW/m^3.

The dryout heat flux as the limiting parameter for the steady state removal of the generated heat by boiling of the coolant was the subject of these investigations. Focus was placed on low porosity, small particle size and relatively large-scale debris beds. A database on the enhancement of dryout heat flux by the CRGT was obtained, for low porosity uniform beds with heat addition of up to 1 MW/m^3.

The scenario of interest is that of the discharge of a large amount of core melt into the lower head of the BWR, which either leads to:

(a) The melt break-up and formation of a large debris bed in water, which may have porosity of 25% to 40%. The lower value of the porosity may result from the very fine particles that may be generated if a small or medium strength steam explosion occurs.

(b) The vaporization of all the water in the lower head resulting in a dry debris bed;

(c) The formation of a melt pool from the dry debris bed.

Further, the three variations of interest for the debris bed and for a melt pool are:

(i) There is no control rod guide tube;

(ii) There is water entry from the bottom into CRGT at the appropriate flow rate and the openings are above the water overlayer;

(iii) The CRGT openings at the top are in the water overlayer, with possibility of water entering from the top.

Several studies of quenching of particle debris beds either by flooding from top or bottom have been reported in the literature [1-4]. Cho and Bova [5] found that during top flooding, the penetration of liquid was faster in the middle of the particulate layer. Ginsberg at al. [6], however, concluded from their experiments that the quenching process was characterized by a two step bi-frontal process with a partial quench front propagating downward and another front traveling upward after the downward front had reached the bottom of the bed. They also proposed a model based on counter-current flooding limitation (CCFL). Tung et al. [7] studied experimentally and analytically the quenching by top flooding when a certain amount of gas was injected at the bottom and heat was generated in the particles. Their model also utilized CCFL.

The purpose of the present work is to study experimentally the effect of the presence of a CRGT in an internally heated homogeneous particle bed on dryout heat flux and quenching processes. The CRGT was modelled with and without water flow.

2.1 POMECO experimental facility

Proper scaling for the experiments is most important; otherwise the data obtained cannot be extrapolated to cover the prototypic situation. We have chosen to represent one CRGT and the debris mass associated like a unit cell. The TVO BWR lower head contains CRGT's at a pitch of 305 mm and the outer diameter of the CRGT is 124 mm with an annular water region of 15 mm width for the bottom 1.4 meters of the lower head, which is the region where the porosity of the bed may be the lowest and it may be most difficult to cool. The decay heat for the scenario would be chosen as that appropriate for 3 - 4 hours after the scram time, i.e.1 MW/m^3.

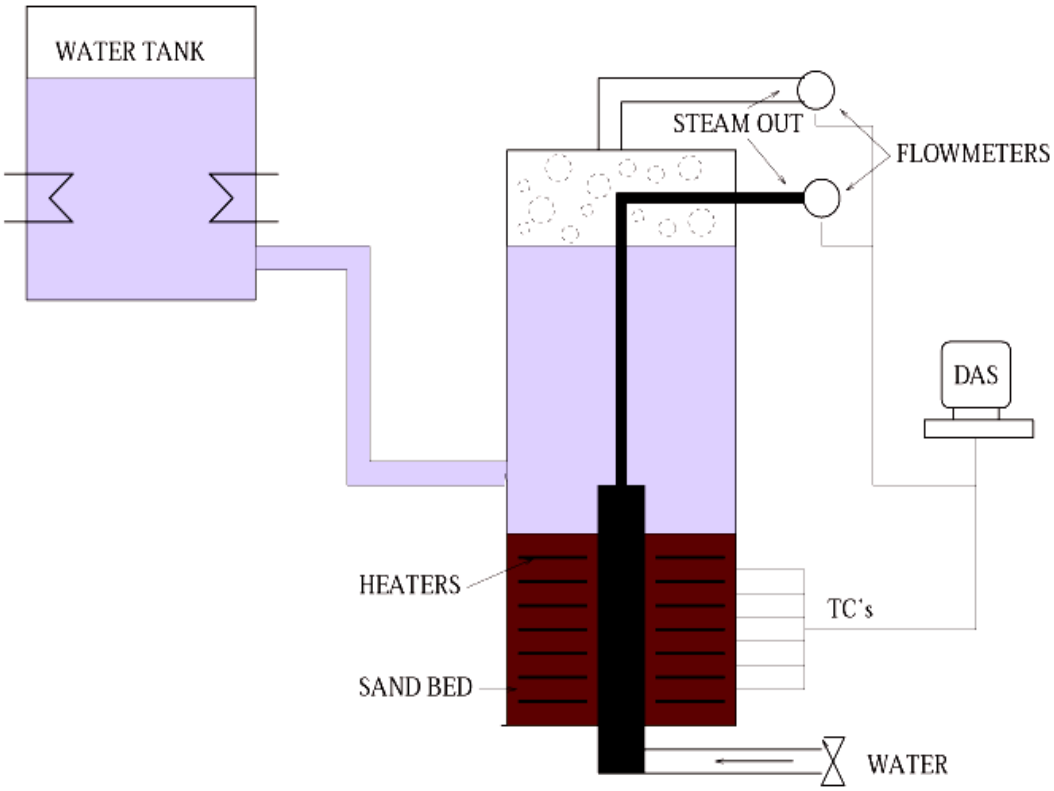

Figure 2.1 POMECO test facility.

The schematic of the modified POMECO (POrous MEdia COolability) facility, designed and constructed at the Nuclear Power Safety Division of the Royal Institute of Technology (Konovalihkin, et al, 1998, 2000), is shown in Figure 2.1. The modification of the POMECO facility employed for earlier debris bed coolability experiments with and without a downcomer consisted of removing the downcomer and constructing a CRGT in the middle of the bed, described in the next section. The POMECO facility consists of water supply system, test section, heater, measurement and DAS systems.

2.2.1 Test section and instrumentation

The test section is a stainless steel vessel whose details are presented in Figure 2.2. The cross-sectional area of the test section is 350×350 mm square. The height of the lower part is 500 mm and the height of the upper part is 900 mm. The maximum height of 370 mm can be obtained for the sand bed. The POMECO facility contains an annular pipe of the same dimensions as the actual CRGT in the BWR lower head (Figure 2.2) inserted into the debris bed.

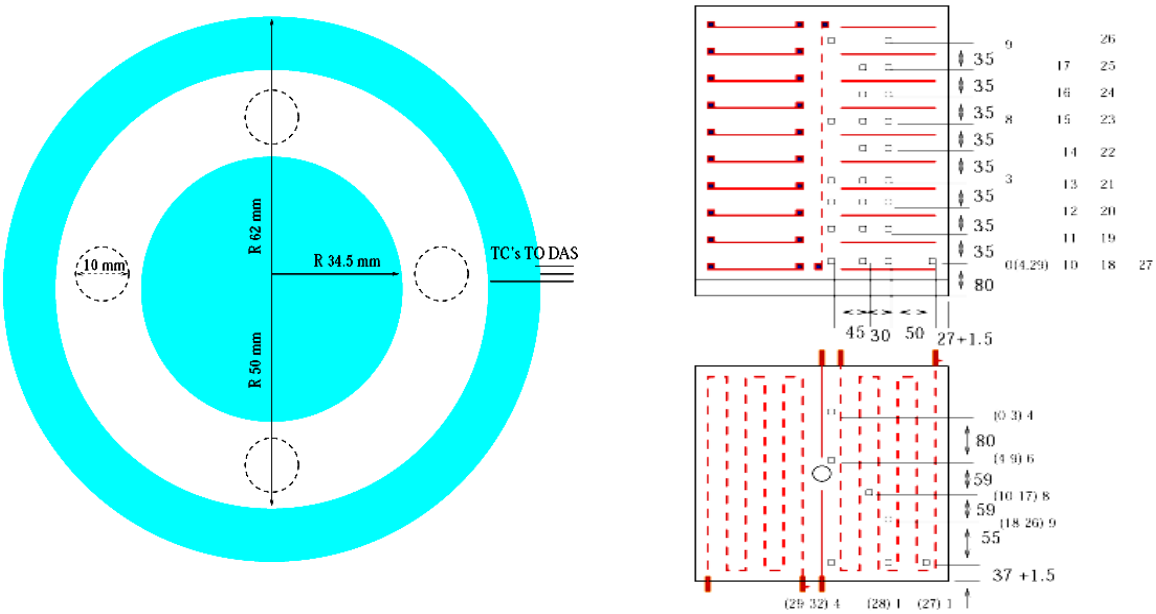

Figure 2.2 CRGT design, heater and thermocouple distribution.

The upper part of the pipe contains holes. These holes are of the same flow area as for the bypass inlet in the prototypic CRGT. The holes are designed to be open or closed. The CRGT annular pipe is led out of the POMECO facility so that the steam generated in the annular pipe can be measured separately from that generated from the water pool. The CRGT pipe is connected to a water line at the bottom which supplies the same rate of water flow to the CRGT as in a prototypic BWR.

The most important measurement in the experiments was the temperature of the sand particle bed. Thirty-three thermocouples were distributed at different positions in the particle bed as shown in the Figure 2.2. The dryout occurrence was recorded according to the readings of those thermocouples. To obtain temperature distribution in the CRGT wall 9 thermocouples were embedded at three different wall depths (Figure 2.2) and at three different positions along the CRGT height.

The steam flow rates were measured using flow meters, installed on the steam lines (as shown in Figure 2.1). The measurement range of these meters is up to 200 liters/sec. From the steam flow rate, the heat removal rate under dryout conditions from the sand bed was evaluated.

2.1.2 Experimental procedure

Tests to determine the dryout power were started with fully saturated bed, before steam flow meter was switched on. The power input to the bed was increased in small steps. Delays of at least 1.5 min were necessary, after a power step, to make reasonable power measurements. Near the expected dryout conditions extremely small power steps were chosen to minimize the overshoot of the heat flux above the dryout heat flux.

The quenching experiments were carried out by establishing a column of water above the dry beds heated up to 450ºC initially, and with the constant internal heat generation during the tests. All the experiments were performed at atmospheric conditions.

2.2 Experimental results

Experiments with the three different bed configurations were performed. The effects of porosity and presence of CRGT on dryout heat flux and quenching rate were measured.

2.2.1 Dryout experiments

The following experiments were planned within each test series on dryout heat flux:

1 No water flow in the CRGT pipe;
2 Water supply flow from the bottom to the CRGT;
3 Water flow through the open upper holes in the CRGT pipe, no water addition from the bottom;
4 Water flow through the open upper annular opening of CRGT, no water addition from the bottom.

In the first two test series (experiment with only top flooding) no dryout at the full power density of 0.98 MW/m^3 was observed (Tables 2.1 and 2.2, Figure 2.3).

Table 2.1 Experimental conditions and results for the sand bed with porosity 0.4 and mean particle size 1.9 mm.

Test	Water flow rate in the CRGT, kg/s	Experimental dryout heat flux, kW/m^2	Dryout heat flux Lipinski model, kW/m^2	
			Without CRGT	With CRGT
DRC-1.1	-	>327	932	1061
DRC-1.2	0.0625 (10°C water)	>327	932	1077
DRC-1.3	0.0625 (85°C water)	>327	932	1094

In the tests DRC-1 this result is confirmed by the Lipinski model, which shows that for such bed configuration dryout can be expected at the power supply of about three times larger than the maximum provided by the POMECO test facility. Experiments with subcooled and saturated water in the CRGT showed similar results.

Table 2.2 Experimental conditions and results for the sand bed with porosity 0.36 and mean particle size 1.0 mm

Test	Water flow rate in the CRGT, kg/s	Dryout heat flux, kW/m^2	Dryout heat flux Lipinski model, kW/m^2	
			Without CRGT	With CRGT
DRC-2.1	-	>327	226	350

In the previous POMECO experiments (test series homo-2 described in [9] for the bed of the same configuration as in the test DRC-2 the measured dryout heat flux was 222 KW/m^2. This result is in good agreement with the prediction by Lipinski model (see Table 2.1). But in the DRC-2.1 experiment with CRGT inside the bed no dryout was obtained (Table 2.2). This can be explained by the additional coolability of the bed, provided by the CRGT. The heat removal rate through the CRGT was estimated as 15 kW, which, added to the Lipinski model value, could provide the estimation of 350 kW/m^2 as the dryout heat flux for these test conditions.

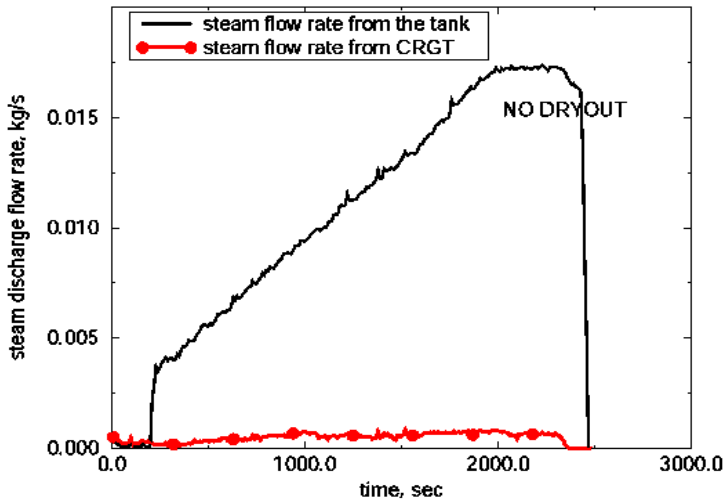

Figure 2.3 Steam discharge flow rate during the tests DRC-1.3

In the third test series the bed with smaller mean particle size than in the previous DRC tests and low porosity of 0.26 was examined. The first experiment, DRC-3.1, showed (Table 2.3) that the presence of CRGT increases dryout heat flux significantly.

Such tests with the same particle bed were conducted during the previous series of POMECO experiments (test series homo-3, see [9]), and good agreement between the experimental results and predictions by Lipinski model was obtained.

From the comparison of these two series of experiments the additional cooling capacity provided by CRGT can be estimated as 10 kW for this bed configuration. It can be seen that addition of this value to the Lipinski model prediction gives a result, which is very close to that from the experiment.

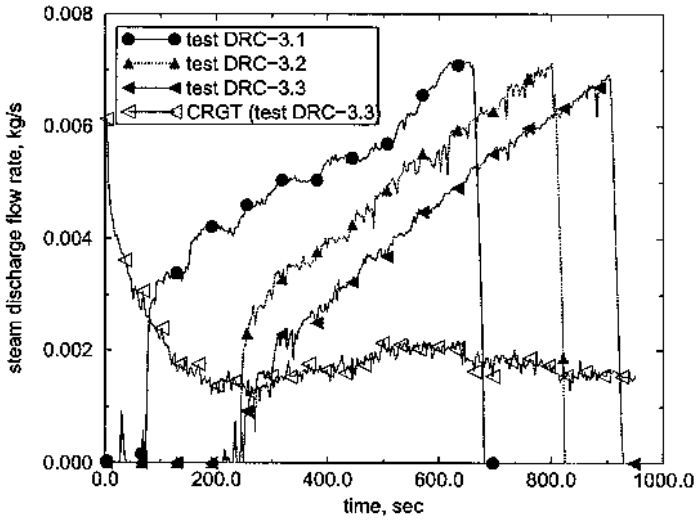

Figure 2.4 Steam discharge flow rates in the tests DRC-3.1, DRC-3.2 and DRC-3.3

The tests DRC-3.2 and DRC-3.3 were conducted to investigate the enhancement of the dryout heat flux by the water flow in the CRGT. Two different water flow rates were tested: 0.0625 kg/s (prototypic) and 0.00625 kg/s both at 85ºC. As it can be seen in the Table 2.3, water flow enhances the dryout heat flux. In the test DRC-3.2 with flow rate of 0.0625 kg/s the additional heat removal is provided due to the heating of flowing water without vaporization. From the experimental data (Figure 2.4) heat flux to the water inside the CRGT is estimated as 30 - 50 kW/m^2.

Table 2.3 Experimental conditions and results for the sand bed with porosity 0.26 and mean particle size 0.8 mm

Test	Water flow rate in the CRGT, kg/s	Dryout heat flux, kW/m^2	Dryout heat flux Lipinski model, kW/m^2	
			Without CRGT	With CRGT
DRC-3.1	-	133	51	132
DRC-3.2	0.0625 (85°C water)	154	51	154
DRC3.3	0.00625	166	51	170
DRC-3.4	Open upper holes	275	-	-
DRC-3.5	Open top part (cross section)	251	-	-

Calculations for the axial distance at which subcooled water becomes saturated (see [10]), are presented in Figure 2.5. They show that 85ºC water, during the test DRC-3.2 does not reach the saturation temperature during its passage through the CRGT (35 cm from the bottom to the top), if the heat flux is in the range of 30 to 50 kW/m^2.

Comparison between experimental result of the test DRC-3.2 and Lipinski model gives good agreement (with accounting of heat removal through the CRGT wall to the water overlayer and heating of water inside CRGT). In the test DRC-3.3 partial vaporization of coolant was registered, which explains higher dryout heat flux in comparison to that in the two previous experiments. To analyze this experiment by the Lipinski model steam generation rate in the CRGT was calculated employing the methodology described in [10]. The results of the comparisons are presented in the Table 2.3.

The objective of the test DRC-3.4 was to investigate dryout behavior in the situation, when saturated water can be delivered into CRGT pipe through the bypass flow openings in BWR. For this purpose four holes, with total flow area (Figure 2.2) equal to that in BWR's bypass, were kept open during this test. As a result (see Table 2.3) a great enhancement in dryout heat flux was obtained. The enhancement may be caused by intensive boiling of the saturated water from the pool inside the CRGT line, which resulted in significantly higher total steam discharge flow rate in comparison to those obtained in the previous tests.

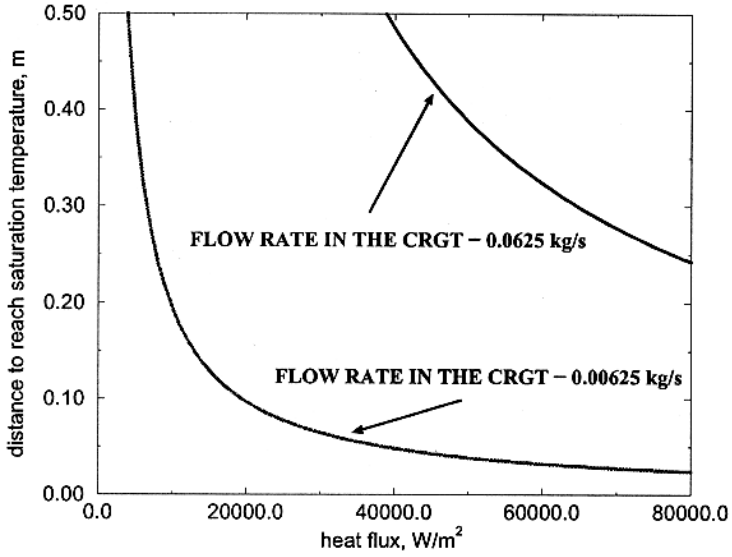

Figure 2.5 Dependence of saturation distance on heat flux (water t=85ºC)

The test DRC-3.5 simulated the situation when the upper part of CRGT pipe is melted down and water can penetrate into the tube through the upper cross-section. The total steam discharge was slightly lower in comparison to that in the test DRC-3.4, and, correspondingly, the experimental heat flux was less (see Table 2.3).

This may be explained by the fact that in the test DRC-3.4 the steam release rates were registered at the outlets of the CRGT pipe and water tank, but in the test DRC-3.5 only water tank steam discharge flow rate was measured, because the upper

part of CRGT pipe was removed, and some part of the steam discharged from the CRGT could be condensed during its passage through the water overlayer.

2.2.2 Dry bed cooling by water flow in CRGT

The experiment DRYFL was performed in order to obtain the heat removal rate from the dry bed by the water flow in the CRGT pipe without top flooding. The objective of this test was to measure heat extraction by water in the CRGT pipe during cooling of the bed from 450°C down to 100°C.

Table 2.4 Experimental results of cooling test for homogeneous particle bed (porosity – 0.4, mean particle size – 1.9 mm); power supply – 4200 W; coolant t=85°C

Test	Initial bed temperature, °C	Water flow rate in the CRGT, kg/s	Average steam discharge flow rate, kg/s	Cooling time, s
DRYFL	450	0.0625 (85°C water)	0.007	4500

Experimental conditions and results of the test are presented in the Table 2.4 and figure 2.6. This test can be characterized by a relatively high heat removal rate by the CRGT, due to a partial vaporization of 85ºC water (see Figure 2.6) during the passage through the CRGT pipe.

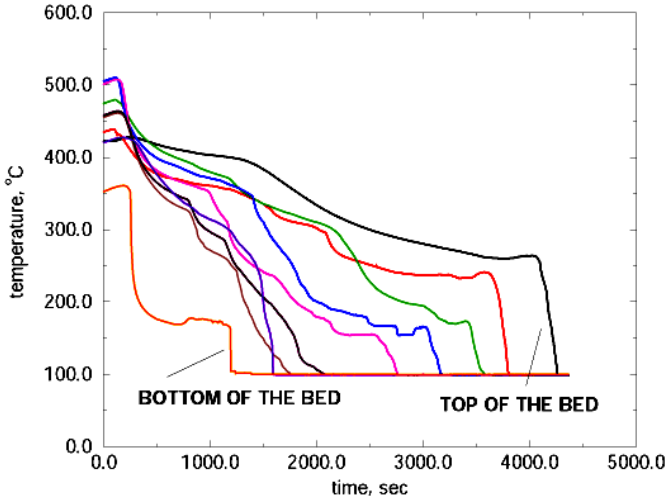

Figure 2.6 Test DRYFL: temperature history

The heat flux was estimated to be 150 kW/m^2. As it can be seen from the Figure 2.7, calculations for the water saturation distance with experimental conditions presented above show that subcooled water cannot reach the saturation temperature. In other words, the dry bed with constant power supply of 4200 W and flow rate in

CRGT of 0.0625 kg/s of 20ºC water will take much longer time to cool down to 100ºC.

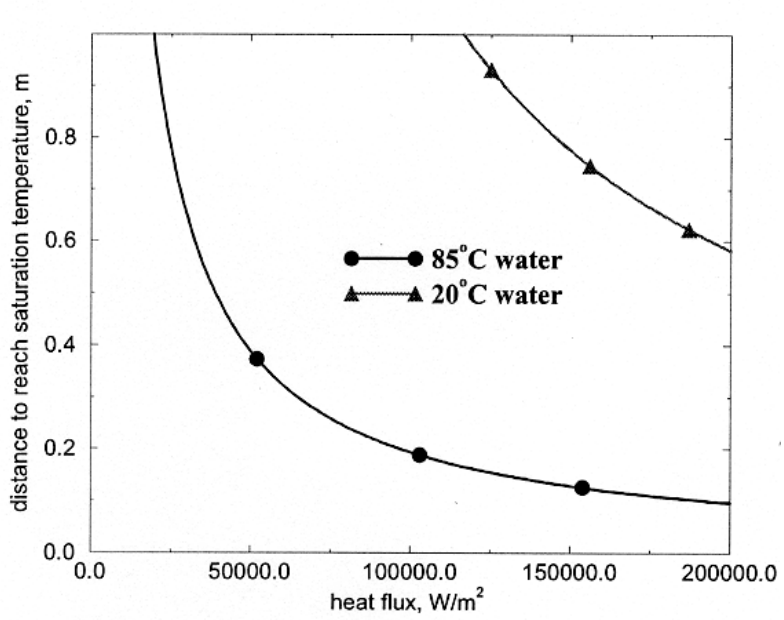

Figure 2.7 Inversely predicted surface heat flux

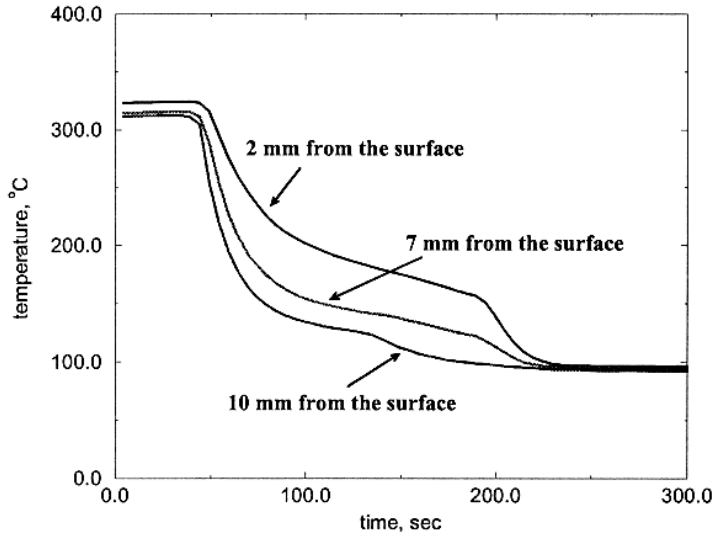

Figure 2.8 Temperature variation in the CRGT wall with depth

The Inverse Heat Conduction Problem (IHCP) is one in which measured temperatures inside a conducting block are used to estimate surface boundary conditions. It is applicable in this CRGT case. Beck's algorithms are employed in a fashion similar to that of CONTA code [12]. Method of 'future time steps' is used and the entire scheme is based upon the minimization of errors between the predicted and measured temperatures.

The variation of temperature inside the CRGT wall at the middle height for the duration of the test DRYFL is given in Figure 2.8.

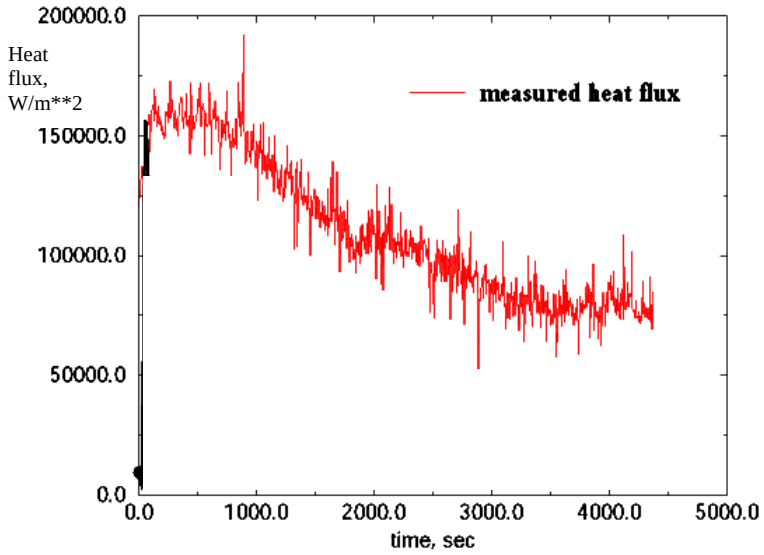

Figure 2.9 Experimental surface heat flux

The experimental surface heat flux is shown in Figure 2.9.

2.2.3 Quenching experiments

2.2.3.1 Experimental results

Three series of experiments with different particle bed configurations were performed to study the effects of porosity and the presence of CRGT on the quenching process of the dry bed. Tables 2.5-2.7 list the experimental results on quenching rates for the homogeneous particle beds with different experimental conditions.

Table 2.5 Experimental results of quenching tests for homogeneous particle bed (porosity – 0.4, mean particle size – 1.9 mm); power supply – 4200 W; coolant temperature – 85ºC

Test	Initial bed temperature, °C	Water flow rate in the CRGT, kg/s	Average steam discharge flow rate, kg/s	Quenching time, s
QC-1.1	500	-	0.014	240
QC-1.2	500	0.0625 (85°C water)	0.02	175

From the temperature histories at various locations in the particulate layer (see Figures 2.10-2.12), the quenching time was determined by a rapid drop in the particle temperature (to about the saturation temperature of water at the system pressure). In all the tests, the mean temperature in the bed was kept the same (500ºC), however, the temperatures in the lower and upper portions of the bed, before quenching, were

slightly lower (400ºC) due to heat losses to environment. In all quenching experiments, described here, the same water overlayer (~0.7 m) was established.

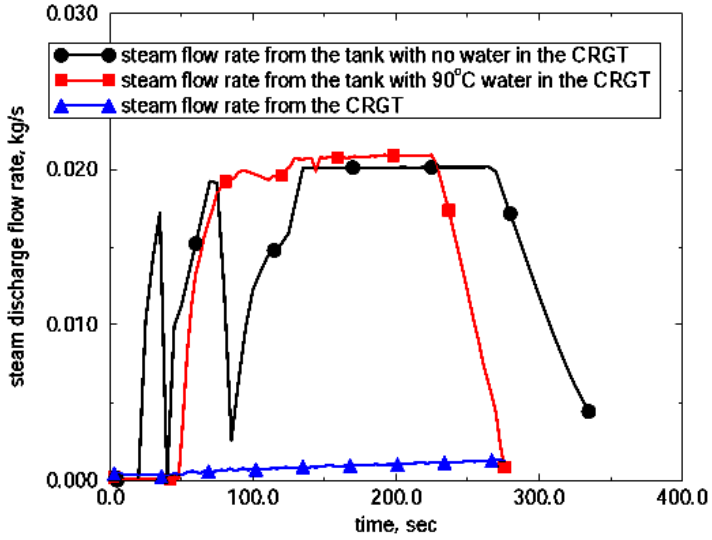

Figure 2.10 Steam discharge flow rates in test QC-1.1

For the particle beds with relatively high porosity value of 0.4 and 0.36 (series QC-1 and QC-2) the quenching rates were high. All these experiments can be characterized by intensive steam generation rates, which are presented in Figure 2.1.

Table 2.6 Experimental results of quenching tests for homogeneous particle bed (porosity – 0.36, mean particle size – 1.0 mm), power supply – 4200 W; coolant temperature – 85 ºC

Test	Initial bed temperature, °C	Water flow rate in the CRGT, kg/s	Average steam discharge flow rate, kg/s	Quenching time, s
QC-2.1	450	-	0.009	210
QC-2.2	450	0.0625 (85°C water)	0.011	160
QC-2.3	450	0.00625 (85°C water)	0.013	140

Water flow in the CRGT pipes slightly decreased the quenching times (Tables 2.5 and 2.6) due to additional heat taken out by the flowing water. In the tests QC-2.2 and QC-2.3 results from two different flow rates are compared: 0.0625 kg/s (prototypic) and 0.00625 kg/s. In the test QC-2.3 with less water velocity more intensive water vaporization was registered, and it caused the greater decrease in quenching time compared to that in the previous test.

Two main observations were drawn from experimental results of QC-3 test series; reported in Table 2.7:

(i) the decrease in porosity resulted in a significant increase of quenching time

(ii) the presence of CRGT in the bed accelerates the quenching process.

The first conclusion was made after the comparison of quenching times in the tests with the same experimental conditions in all test series (Tables 2.6 and 2.7).

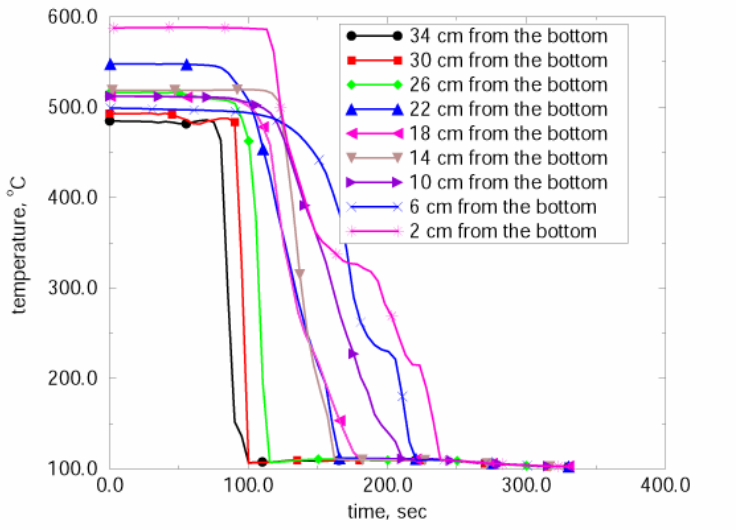

Figure 2.11 Quench front propagation in the test QC-2.1

In these tests the mean particle sizes were quite similar, but porosity value in the test series QC-3 was lower. It led to the slower water penetration through the bed because of higher capillarity (Table 2.7 and Figure 2.12). The initial peak in the steam generation the Figure 2.12 occurred at the instant when the water was supplied to the top of the debris bed. High steam production rate was achieved due to direct contact heat transfer between water and the hot debris bed. Afterwards, as the water was supplied at a subcooled temperature (of about 85°C), the subcooled liquid in the tank had to be heated up to the saturation temperature. The high steam generation rate was resumed after the bulk liquid temperature reached the saturation value in the tank (at about t=300 sec).

The second conclusion was drawn from the comparison of experimental results of the tests QC-3.1 and QH-2.1 conducted during the performance of quenching experimental program described in [10]. The presence of CRGT inside the bed decreased the quenching time by a factor of two. This effect of CRGT is similar to that of a downcomer (3 cm in diameter), which can deliver water from the top to the bottom, employed in the previous quenching program.

Table 2.7 Experimental results of quenching tests for homogeneous particle bed (porosity – 0.26, mean particle size – 0.8 mm), power supply – 4200 W; coolant temperature – 85 ºC

Test	Initial bed temperature, °C	Water flow rate in the CRGT, kg/s	Average steam discharge flow rate, kg/s	Quenching time, s
QC-3.1	450	-	0.003	1300
QC-3.2	450	0.0625 (85°C water)	0.0035	1200
QC-3.3	450	0.00625 (85°C water)	0.004	1100
QC-3.4	~470	Open upper holes	0.007	1000
QC-3.5	450	Open upper cross section	0.005	950

.

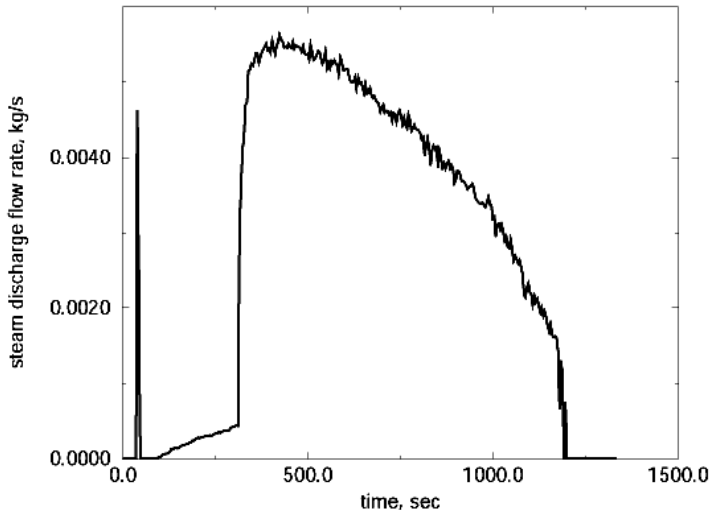

Figure 2.12 Steam discharge rate in the test QC-3.1

The test QC-3.4 was performed with open upper holes, which are simulating BWR's bypass openings. Through these holes saturated water from the water overlayer penetrated in the CRGT pipe and provided intensive boiling inside the pipe with intensive steam release (Figure 2.13).

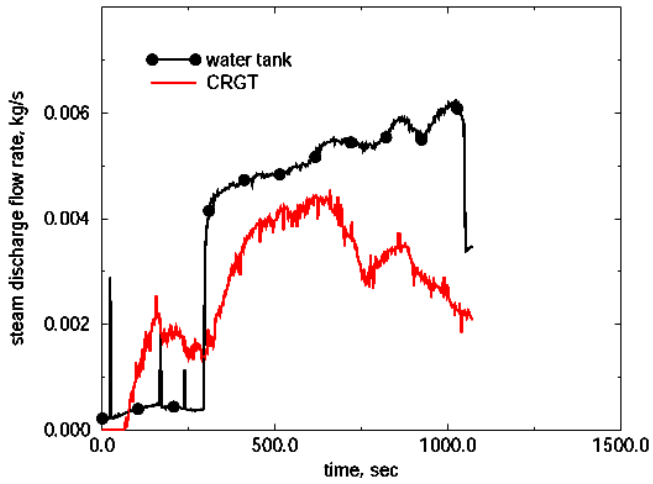

Figure 2.13 Steam discharge rate and quench front propagation in the test QC-3.4

It did not lead to significant decrease in quenching time because the initial bed temperature was higher in comparison to that in previous tests of this series. The last quenching experiment QC-3.5 with the open annular cross-section represented the situation with melted down upper part of CRGT. The test showed that the larger flow area provided greater water penetration into CRGT and, thus, provided greater heat transfer, which led to the decrease in quenching time (Table 2.7) in comparison to that in the previous experiments of this test series.

2.2.3.2 Analysis

A simple zero-dimensional integral analysis has been performed based on the consideration of hydrodynamic flooding due to steam formation (see [10]). The basic assumptions are that the penetration of the quench water is uniform across the bed cross section and the steam is generated immediately after contact of water with the solid particles, and that the steam heats up the water overlayer. In addition, it is assumed that the hot particles are completely quenched and cooled to water saturation temperature as the water penetrates in the bed. The quenching rate of the bed is directly proportional to the penetration rate. The following relation for the quenching time can be written:

$$\Delta t = \frac{\rho_{sol} C_{p,sol} (1-\varepsilon) V (T_{sol} - T_{sat})}{(G_w H_{fg} + W_{CRGT}) - W}$$

Here, heat removal rate through CRGT W_{CRGT} consists of heat removed through CRGT structure (wall) to the water overlayer, heat to heat up water inside the CRGT: $G_{w,CRGT}\Delta T$ and heat of water vaporization $G_{w,CRGT}H_{fg}$. The numerator in this ratio is responsible for the total heat, which has to be removed in order to quench the bed and the denominator is the cooling down (quench) rate.

To estimate heat removal rate through the CRGT structure CONTA code was employed. The results of calculations are presented in the Figure 2.14. It can be seen that for given experimental conditions the CRGT surface heat fluxes are between 100

KW/m^2 and 170 KW/m^2. Higher heat flux in the QC-1.1 test is provided due to the higher initial bed temperature.

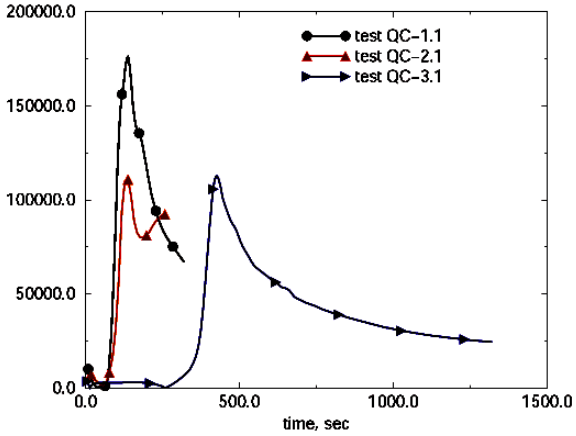

Figure 2.14 Inversely predicted surface heat flux in quenching experiments QC-1.1, QC-2.1 and QC-3.1

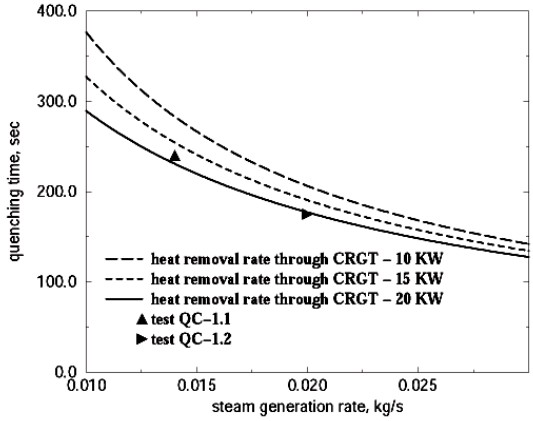

Figure 2.15 Comparison between experimental and calculated results of QC-1 test series

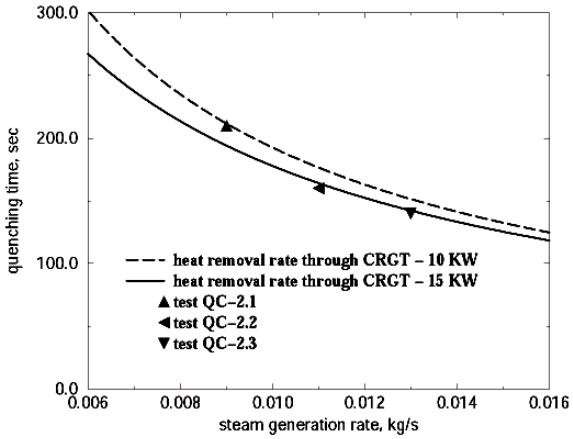

Figure 2.16 Comparison between experimental and calculated results of QC-2 test series

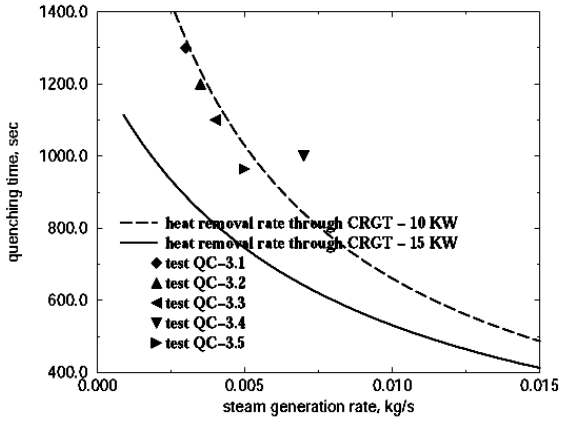

Figure 2.17 Comparison between experimental and calculated results of QC-3 test series

Using the method described in [10] and values predicted by the CONTA calculations all the quenching experiments performed in these three test series were analyzed. The results of the analysis are depicted in Figures 2.15 and 2.16. As it can be seen from these Figures the experimental results of the first test series agree best with the calculations, with average heat removal rate through CRGT structure taken as 20 kW, second test series - between 10 and 15 kW, and last one - 10 kW.

2.3 Conclusions

In this report, experiments, performed at RIT (Royal Institute of Technology), on the dryout heat flux and quenching rate with three different configurations of the porous particulate bed and different cooling regimes have been presented.

It was found that the presence of the control rod guide tube provides a significant additional cooling capacity for the bed, which leads to enhancement of dryout heat flux and the quenching rate. Heat removal rate through CRGT structure was found to be 10 - 15 kW depending on surrounding porous media and temperature regime. Water flow rates in the CRGT result in additional enhancement of dryout heat flux and intensification of quenching process.

Lipinski model with addition of coolability potential of CRGT was employed to analyze dryout experiments. Reasonable agreement between experiments and calculations was obtained.

Characteristic times for quenching were computed by the model, which combines parameters of the process (V, p_{over}, T_{sol}, T_w, W), geometry (A_{bed}, d_{dwnc}) and physical properties (H_{fg}, $C_{p,w}$, ρ_w, μ_w, $C_{p,sol}$, ρ_{sol}, ε). Good agreement between experimental and calculated results has been achieved.

3. COMECO experiments

3.1 Introduction

A series of experiments on COMECO (COrium MElt COolability) test facility were carried out in order to further assess the heat removal efficiency of the CRGT. The COMECO test section was subjected to higher temperatures, compared to those in the POMECO test facility. The cross sectional area of the test section was 200×200mm, maximum melt height was up to 300 mm. A binary oxide mixture (30%CaO-70%B_2O_3) was employed as a simulant corium material at the COMECO test facility. The temperatures at the test section were up to 1100°C. Three series of experiments were performed with two different CRGT configuration:

i) Closed bypass openings at the upper part of the CRGT. The coolant was supplied at different flow rates (6.25÷62.5 g/s) and at different temperatures (20°C and 95°C).
ii) Flow through the CRGT at various coolant temperatures (20°C and 95°C) and various coolant flow rates (6.25÷62.5 g/s) and the open bypass at the upper part of the CRGT.

Series of quenching experiments were carried out, while establishing a water layer on the top of the molten pool. The objective of the COMECO experiments was to evaluate the heat removal capacity of the CRGT's with a high temperature melt that can form a crust layer on the outside surface of the CRGT.

3.2 Molten pool simulant material selection

Experimentation and analysis were conducted at the Division of the Nuclear Power Safety (NPS), KTH during the previous years (Stolyarova, V.L., Green, J., 1997) in order to determine a suitable material for the UO_2-ZrO_2 (corium) simulant material. The safety concerns associated with employing the actual corium (UO2-ZrO_2-Zr) material preclude conduct of such experiments with an actual UO_2-ZrO_2 mixture. However, using proper scaling techniques (such as solidification rate, density, diffusivity and temperature ratios, freezing number, time separating short from long term solidification, sparging gas rate, surface orientation, non-dimensional ratio of latent heat/stored heat) it was possible to choose the proper simulant for corium. After a series of investigations a binary mixture of calcium – boron oxide (30%CaO-70%B_2O_3) was chosen to be the simulant corium material for the COMECO experiments. The selection was done on the basis of similarity of this binary oxide to the corium (which is 80%UO_2-20%ZrO_2) in the terms of phase diagram (Figure 3.1), which is similar to the UO_2-ZrO_2 phase diagram for the difference between the liquidus and the solidus temperatures. Table 3.1 presents some physical properties of corium (UO_2-ZrO_2) and some available corium simulant

materials. About 11 liters of the CaO-B_2O_3 melt were poured into the test section of the COMECO facility during the experiments.

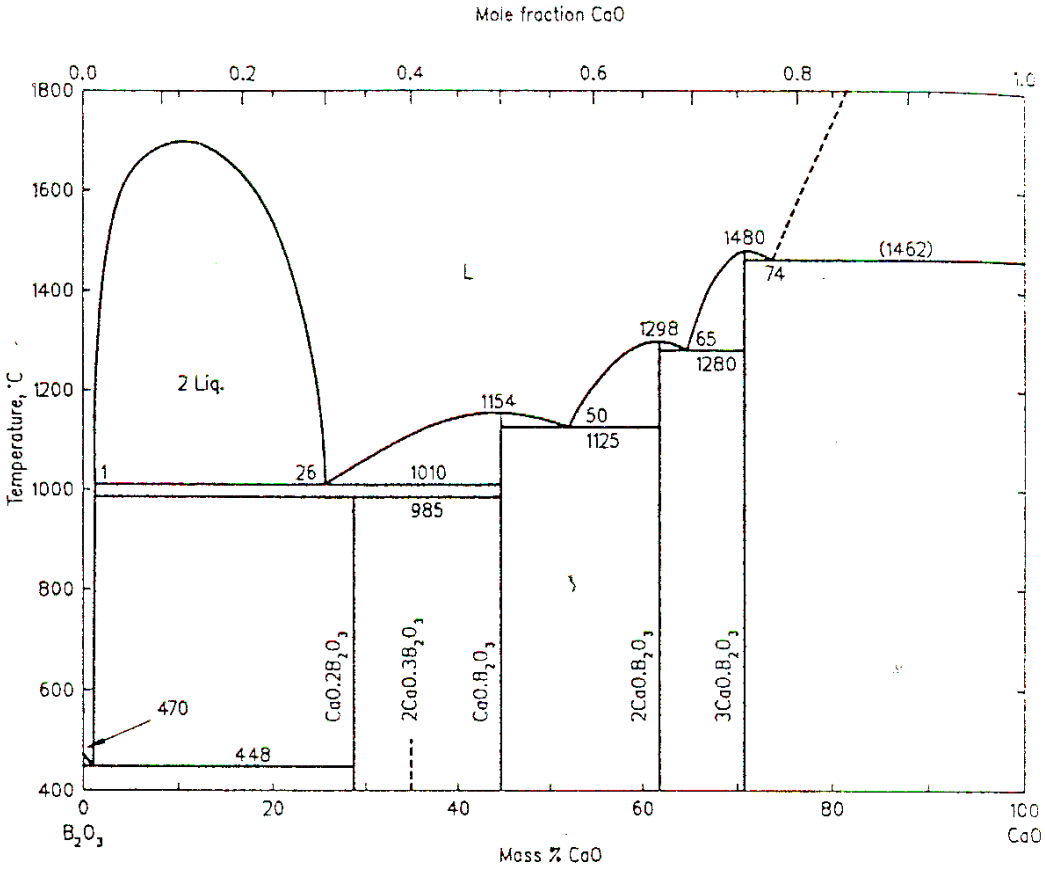

Figure 3.1. Phase diagram of the CaO-B_2O_3 system

Table 3.1. Physical properties of corium and simulant materials

PROPERTY	Corium (UO_2 – ZrO_2) (80 – 20 Wt%)	CaO – B_2O_3 (30 – 70 Wt%)	MnO - TiO_2 (78 – 22 Wt %)	CaO – WO_3 (5 – 95 Wt %)	Al_2O_3
Melting point (K)	2900	1300	1650	1525	2300
Density (Kg/m^3)	8000	2500	4500	6500	2500
Viscosity (Pa.s)	0.005	0.1 – 0.3	------	------	0.004
Thermal Conductivity (W/m/K)	10	3.0	------	------	8
Surface tension (N/m)	1.0	0.15	------	------	0.5
Specific heat (J/Kg/K)	540	2200	900	500	775
Fusion heat (KJ/Kg)	360	460	------	70	1000

3.3 Test section

3.3.1 Scaling of the test section

The dimensions of the COMECO facility are smaller than the dimensions of the corresponding unit cell of the prototypic BWR. Therefore a proper scaling relation had to be introduced in order to maintain the correct representation of the experiment setup, compared to the prototypic case.

The scaling down of the CRGT model, employed in the COMECO test facility was done by maintaining the same ratio:

Heat transfer area / Flow area = Const

The area of the bypass openings was also reduced according the ratio:

Bypass area / Flow area = Const

3.3.2 COMECO facility

The schematic diagram of the COMECO facility is shown in the Figure 3.2.

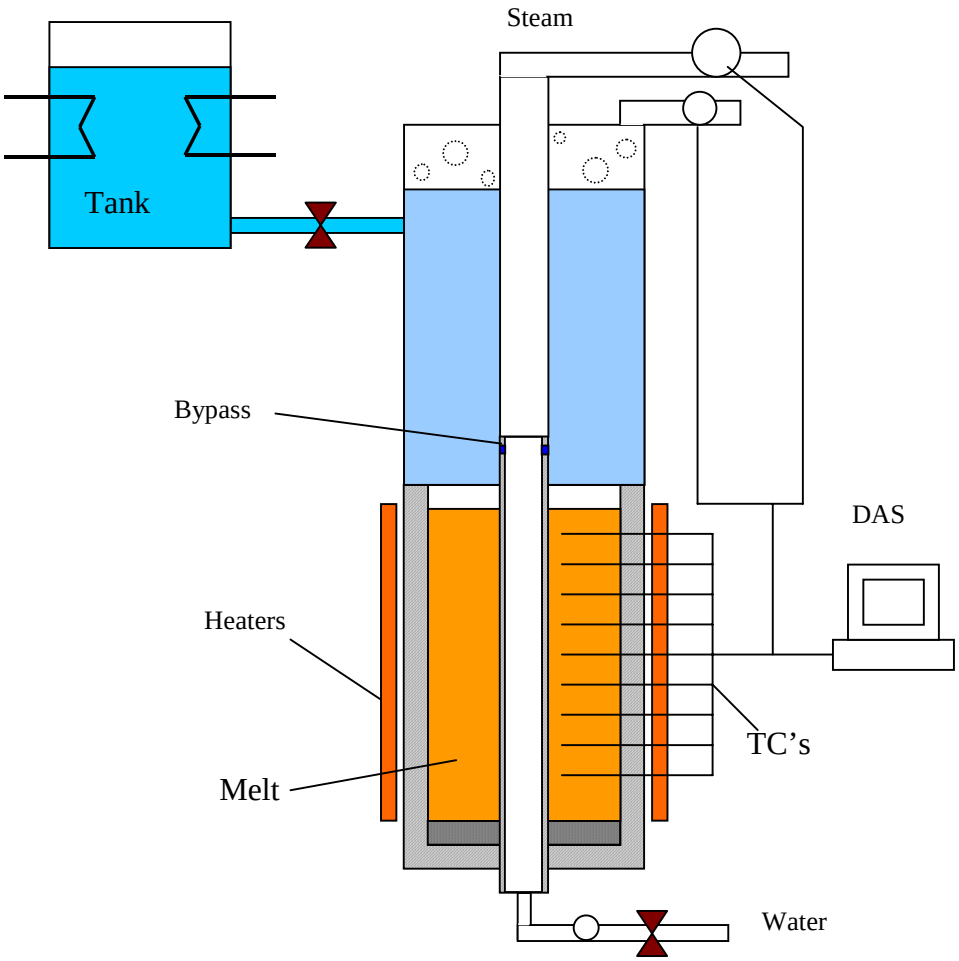

Figure 3.2 COMECO test facility

COMECO facility (Figure 3.2) consisted of a test section (200 × 200 mm cross section), with the maximum of 300 mm of melt height. The test section walls were made from 25 mm thick carbon steel and 24 thermocouples were placed within the test section. The test section was connected to the upper tank (1000 mm high). Water was supplied to the upper tank via the water line from the heated water storage. A water level gauge was installed in the upper tank to monitor the water level variation during the experiments.

The CRGT model (with the outside diameter d_o=50 mm and the inside diameter of d_i=45 mm) was placed in the centre of the test section. The CRGT was connected to the water line at the bottom. Water at different subcooling temperatures could be supplied through the water line. Two bypass openings (of the diameter d= 9 mm) were made in the upper part of the CRGT model.

Two flowmeters were installed on the steam outlet lines from the CRGT and the upper tank. A flowmeter was installed also on the water supply line, to measure the water flowrate through the CRGT.

3.3.3.1 Heating system

In the COMECO facility, the melt layer was heated directly by KANTHAL heaters, located on the sidewalls of the test section. Four heaters were installed on the four sides of the test section. The maximum power of 16 kW could be delivered to the melt pool. Thus, the COMECO experiments could be conducted at the maximum power density of 1.33 MW/m^3.

3.3.3.2 Water supply system

Water to the upper tank was supplied from a water supply tank. During the experiment, the valves on the water supply lines were opened as the quenching experiments started. After water reached a certain level (close to the top of the upper tank) the line was closed. The water level gauge indicated the remaining level of water during the experiment. When the water level in the upper tank was approaching the lower level limit (close to the mid-section of the upper tank), the water level gauge generated a signal and the water supply line was re-opened to refill the tank with water. Water at 95°C was used in the series of COMECO experiments for the top quench of the melt pool.

3.3.3.3 Instrumentation and data acquisition system (DAS)

The most important measurements during the experiments were the melt temperatures at various locations within the melt pool. The temperature readings were obtained from 24 thermocouples, uniformly distributed within the melt pool. The thermocouples were placed at 8 axial elevations and at 3 radial locations in the melt pool. The distribution of the thermocouples in the COMECO facility is shown in the Figure 3.3.

The steam flow rates, generated within the CRGT and the upper tank, were measured by the two Vortex type flowmeters made by Omega company. The measurement range of the flowmeters was up to 200 litre/sec. The heat removal rate was evaluated from the steam flow rate from the CRGT and the upper tank.

The CRGT water flow rate was also measured used a liquid/gas flow meter, produced by the Omega company.

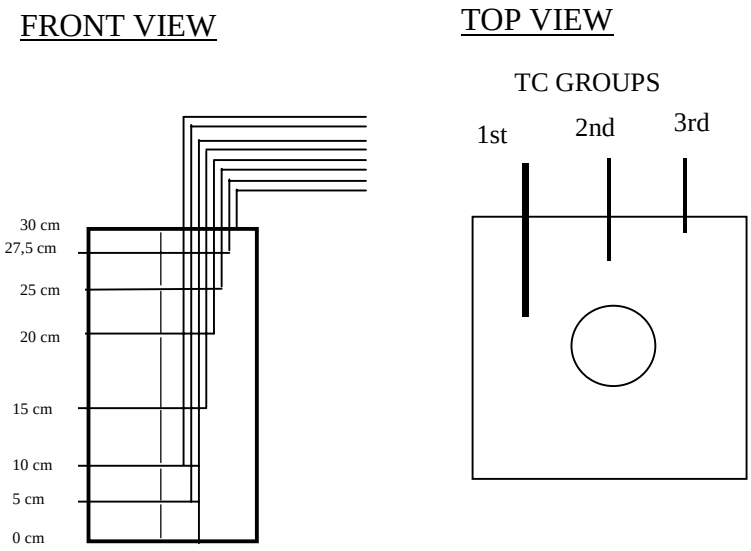

Figure 3.3 Thermocouple distribution in the COMECO facility

All the above parameters (temperatures and flow rates) were registered by the data acquisition system and were saved using HP VEE DAS software.

3.3.4 Experimental procedure

Before the experiment, the binary oxide mixture was heated up to the initial temperature of about 1300°C. The test section was also heated up to about 1000°C in order to avoid the thermal shock and deformations of the test section when the melt was poured. After this the melt was poured into the COMECO test section and the test section was further heated (up to 1100°C). Afterwards the requisite coolant flow rate was established through the CRGT and the experiments were started.

3.4 Experimental results

Three high temperature coolability experiments were carried out at COMECO facility for the melt pool with a CRGT inside. As the experiments were performed at high temperatures (up to 1100°C), and the test section materials were subjected to a severe environment, attempts were made to complete the various phases in the same experiments. Thus each experiment employed different CRGT flow rates, with different inlet temperatures and with/without the top quenching of the melt pool.

The first experiment (CT-1) in the series was performed with closed bypass openings at the top of the CRGT. The second experiment (CT-2) was performed with different flow rates and coolant temperatures in the CRGT (during this experiment the test section had failed and the melt had leaked, therefore the experimental data from this test are not reliable). The third experiment was performed with open bypass holes and with flow in the CRGT.

3.4.1 Experiment CT-1

The first experiment in the series (CT-1) was performed with closed upper bypass holes in the CRGT. In the first phase of this experiment (Table 3.2), the coolant was supplied at ~11°C and at the flow rate of 62.5 g/s (nominal flow rate in the reference BWR). After that the flow rate was reduced to 6.25 g/s. As the feed water was highly subcooled, only its partial evaporation occurred during its passage in the CRGT in the Phase I of this experiment. Reduction of the coolant flow rate led to greater evaporation in the CRGT but the overall heat removal rate was reduced, due to the significantly lower mass flow rate during the Phase II and to the fact, that the melt pool temperatures were lower during the Phase II (Figure 3.6), compared to the Phase I.

Table 3.2 Experiment CT-1

Phase	Flow rate in CRGT, g/s	T_{water} in CRGT, °C	Top flooding	Time on DAS, s
I	62.5	11	NO	112
II	6.25	11	NO	590
	Flow stopped			700
III	6.25	95	YES	3200

During the Phase II of this experiment, the CRGT feed water temperature was raised to 95°C (at a flow rate of 6.25 g/s). At the same time, the water was supplied to the top of the melt pool (the water temperature was 95°C).

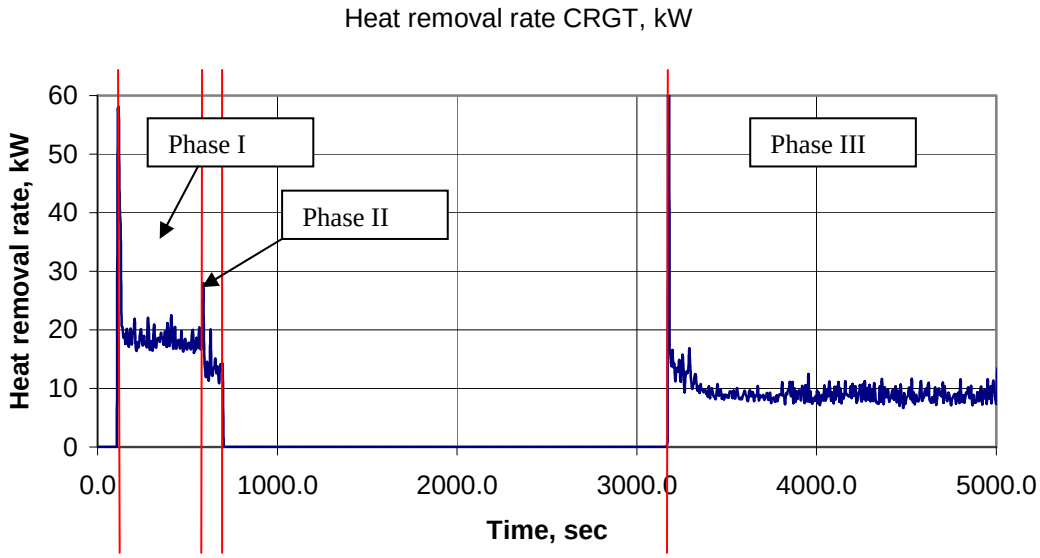

Figure 3.4 Heat removed through CRGT during the experiment CT-1

The heat removal rate from the CRGT and from the upper tank, for the three phases of the experiment CT-1 were based on the steam flow rates obtained from the steam flow meters. The total heat removed was estimated as a sum of the heat, required to heat up the water to the saturation temperature and the latent heat of vaporization.

As seen from the Figure 3.4, the reduction of the flow rate through the CRGT from 62.5 g/s to 6.25 g/s (Phase I-II) led to a decrease of the heat removal rate (from 18 kW removed through the CRGT at 62.5 g/s flow rate to 11 kW at 6.25 g/s). During phases I and II a highly subcooled liquid (11°C) was supplied to the test section, therefore, the evaporation rate was low for these phases of the experiment. During the Phase III slightly lower heat removal rates were registered (Figure 3.4), even though the feed water temperature was close to saturation and much greater evaporation rates were expected. But the additional top flooding during the Phase III (Figure 3.5) decreased the average melt pool temperature, therefore decreasing the overall heat transfer coefficient to the CRGT. For the Phase III the amount of heat removed through the CRGT was about 10 kW (at the coolant flow rate of 6.25 g/s through the CRGT).

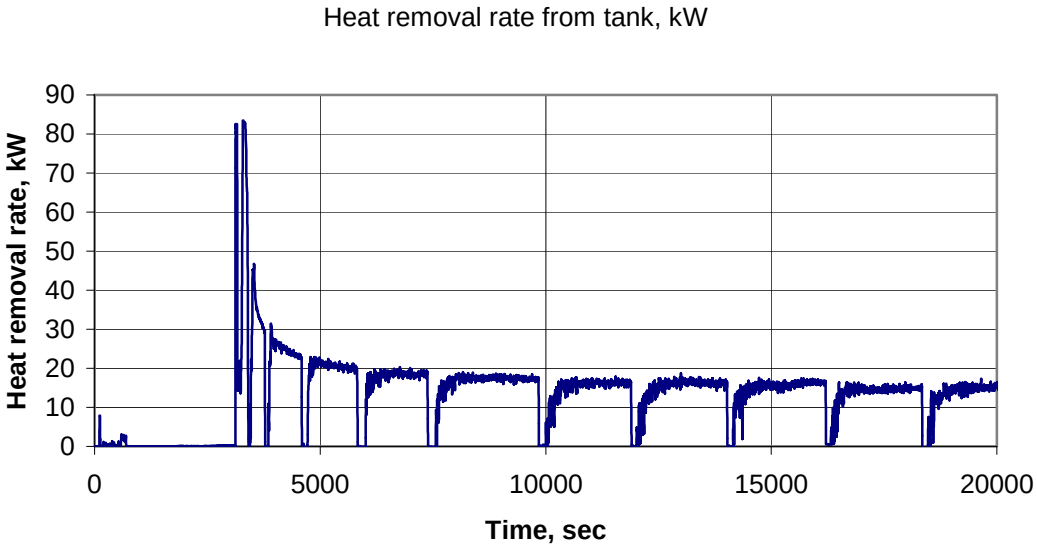

Figure 3.5 Heat removed from tank during the experiment CT-1

Figure 3.5 shows a high heat removal rates (up to 80 kW) from the upper tank at the beginning of the quenching process. However, due to the rapid crust formation at the upper layer of the melt pool, the heat transfer rate to the water in the tank decreased exponentially and stabilized at about 18 kW for the later stages of the experiment. The cyclic behaviour of the heat removal rate from the tank in the Figure 3.5 could be explained as follows: during the experiments, the upper tank had to be refilled with coolant at a certain time intervals, because the water was evaporating from the tank. A slightly subcooled liquid was supplied at the top of the melt pool (at t=95°C), therefore it took several seconds to reheat the liquid in the tank to the saturation temperature and to restore the steam flow from the tank.

During the COMECO experiments, full quench of the melt pool was not achieved. This supports the findings of other experimental programs (e.g. MACE program carried out at the Argonne National Laboratory (with corium: UO_2-ZrO_2 melt), during which the full quenching of the pool was also not achieved due to the formation of an impermeable crust on the top of the melt pool.

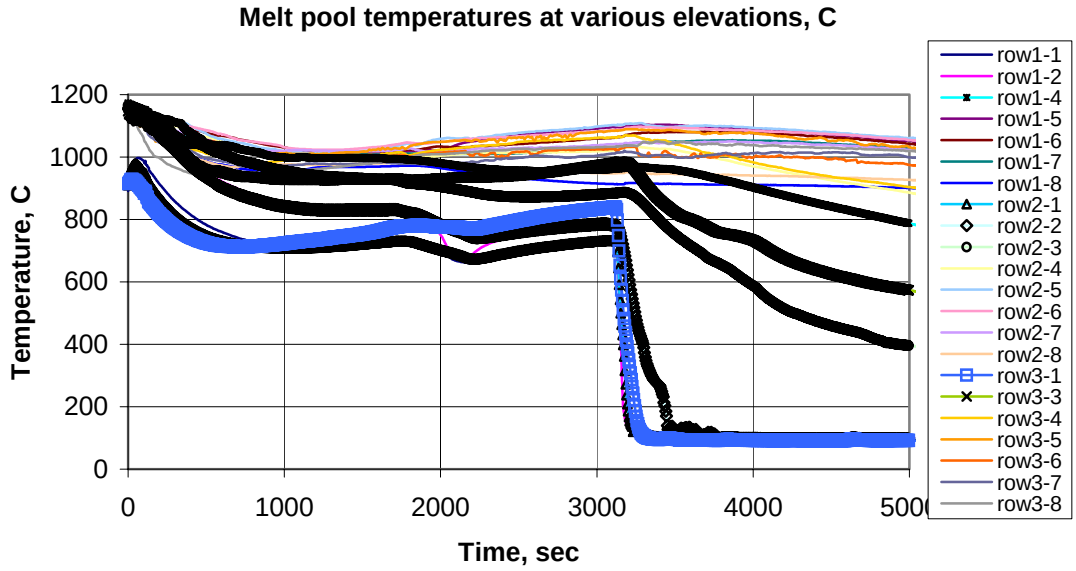

Figure 3.6 Melt temperature distribution during the test CT-1

Figure 3.6 presents the melt temperature histories measured during the test CT-1 by the 24 thermocouples. The thermocouples were placed within the melt pool at 3 radial locations (or rows, see Figure 3.3). The thermocouples were numbered from the top of the melt pool (e.g. the series row1-1 means the 1st thermocouple from top in the group 1, etc.). The melt temperature was reduced by about 300 °C during the Phase I and II of the experiment (no top quenching) for the first 2 top levels with the thermocouples. For the rest of the melt pool, the temperature reduction during the first 2 phases of the experiment was of a magnitude of about 200°C. The temperature reduction at the upper layers of the melt pool during the t=1800-2200 seconds was due to the fact, that the wall heaters were temporarily turned off during this time, as the wall temperatures for the test section were exceeding the maximum values for the thermocouple readings (1150 °C), therefore the heat input had to be reduced in order to avoid the damage to the test section. After t=2200 sec the heaters were set back to the nominal power of 16 kW again.

At about 3200 second of the experiment (Figure 3.6), water was added to the top of the melt pool. Two top levels with thermocouples were quenched immediately after the water was supplied. i.e. the upper part (of up to 5 cm thick) had formed a permeable particulate debris on the top of the melt pool. As the crust thickness continued to grow during the experiment, the melt temperature was continuously decreasing (due to a conduction through the crust). The thermocouples in 3rd and 4th layers also indicated cooling of the melt, i.e. sufficient cooling was achieved in about 10 cm deep layer of the binary oxide melt pool due to water ingression and heat conduction to the water overlayer through the crust (although only upper 5 cm of the melt pool formed debris bed of various size particles were permeable to coolant).

In the lower parts of the melt pool (deeper than 10 cm), temperatures were also reduced, although slowly, which points out that the heat removal rate was higher than the heat addition rate, but the cooling down process was very slow and

temperatures in the middle and lower part of the test section still remained above 600°C at the end of the experiment (about 7 hours from the beginning).

The results of the experiment are summarized in the Table 3.3. From the results, it may be concluded, that the maximal heat removal rate from the test section could be up to 80 kW (at the early phases of the process). After the crust at the top of the melt pool is formed, about 28 kW of heat were removed from the test section by both the top quenching (heat transfer through the crust) and flow through the CRGT. The maximal heat removal capacity of the CRGT was 18.0 kW.

Table 3.3 Summary of the experiment CT-1

Phase	Flow rate in CRGT, g/s	T_{water} in CRGT, °C	Top flooding	Heat removed through CRGT, kW	Heat removed by top quenching, kW	Total amount of heat removed, kW	Average heat transfer coefficient at CRGT wall , kW/m²
I	62.5	11	NO	18.0	-	18.0	382
II	6.25	11	NO	11.0	-	11.0	233
III	6.25	95	YES	10.0	83÷18	93÷28	212

3.4.2 Experiment CT-2

The second experiment in the series (CT-2) was planned to be carried out with the closed bypass openings and with various coolant flow rates and temperatures in the CRGT. Unfortunately, the experiment was not completed, as the test section developed a leak and all the melt was lost to surroundings.

3.4.3 Experiment CT-3

The third experiment in the series (CT-3) was performed with open upper bypass in the CRGT. This experiment consisted of 5 phases. Figure 3.7 shows the steam flow rates from CRGT and tank during the experiment.

After the Phase I, II and III, the test section was reheated to high temperatures and the experiment continued. In the first phase of this experiment (Table 3.4), the coolant was supplied at ~12°C and at the flow rate of 62.5 g/s (nominal flow rate in the reference BWR). As the bypass holes were open above the melt pool, part of coolant was supplied to the upper tank of the COMECO facility on the top of the melt pool through these openings. This generated additional steam flow from the tank and provided additional coolability capacity for the melt pool.

Table 3.4 Summary of the experiment CT-3

Phase	Flow rate in CRGT, g/s	T_{water} in CRGT, °C	Top flooding	Time on DAS, s
I	62.5	12	NO	280
End of Ph. I				880
II	6.25	12	NO	3980
End of Ph. II				4570
III	62.5	95	NO	7480
End of Ph. III				8100
IV	6.25	95	NO	12880
V	6.25	95	YES	13480

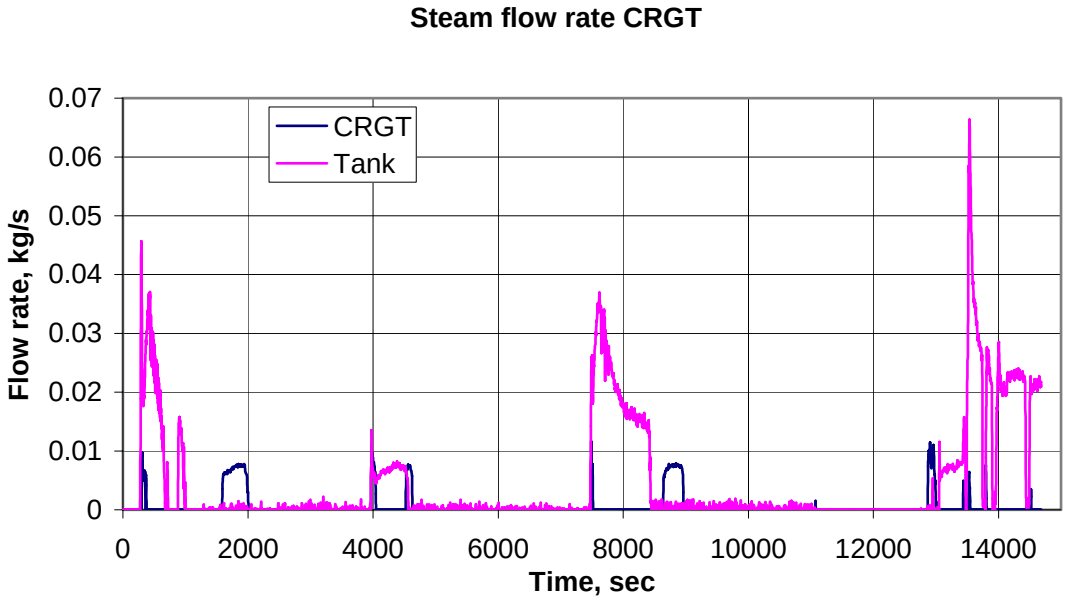

Figure 3.7 Steam flow rates during experiment CT-3

In the second phase of the experiment the flow rate through the CRGT was reduced to about 6.25 g/s. During the third phase the coolant at t=95ºC and flow rate of 62.5 g/s was supplied to the CRGT. In the Phase IV the coolant flow rate was reduced to ~6.25 g/s. The actual coolant flow rate to the CRGT during the Phases II and IV was fluctuating between 6-9 g/s. In the Phase V additional water was supplied to the upper tank and melt pool quenching (with additional flow of the water through CRGT) was investigated.

3.4.3.1 PHASE I

At t=280 sec from the beginning of the experiment, water at t=12ºC with flow rate 62.5 g/s was supplied to the CRGT (Figure 3.8 and 3.9). During the first seconds of the process, high heat removal rates from both CRGT and upper tank were recorded. Since the water at a low temperature and high flow rate was supplied, after the initial peak at about t=300 s, the heat removal rates decreased, as the upper layer of melt in the tank was under a layer of the subcooled water, supplied through the

bypass holes in the CRGT. At about t=330÷340 sec the water layer over the melt pool reached the saturation temperature and higher amounts of steam were generated in the upper tank.

The heat removal rate from CRGT was more than 35 kW during the first 100 seconds of this experiment Phase. Later on, no steam generation in the CRGT was recorded by the DAS. This could be explained by the formation of the crust and reduction of the heat transfer coefficient in the proximity of the CRGT wall within the test section at the later stages of the Phase I. Also, as the upper tank and the CRGT volumes were interconnected via the bypass lines, it is probable that the steam, generated within the CRGT in the later stages of the Phase I (and similarly in the other Phases of the experiment CT-3) was escaping into the tank vessel.

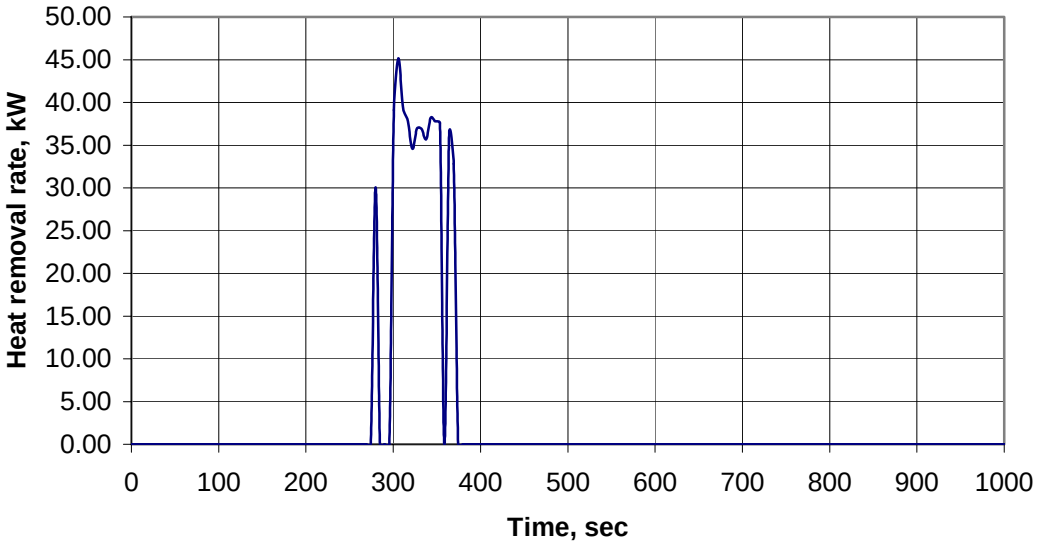

Figure 3.8 Heat removed through CRGT during the experiment CT-3, Phase I

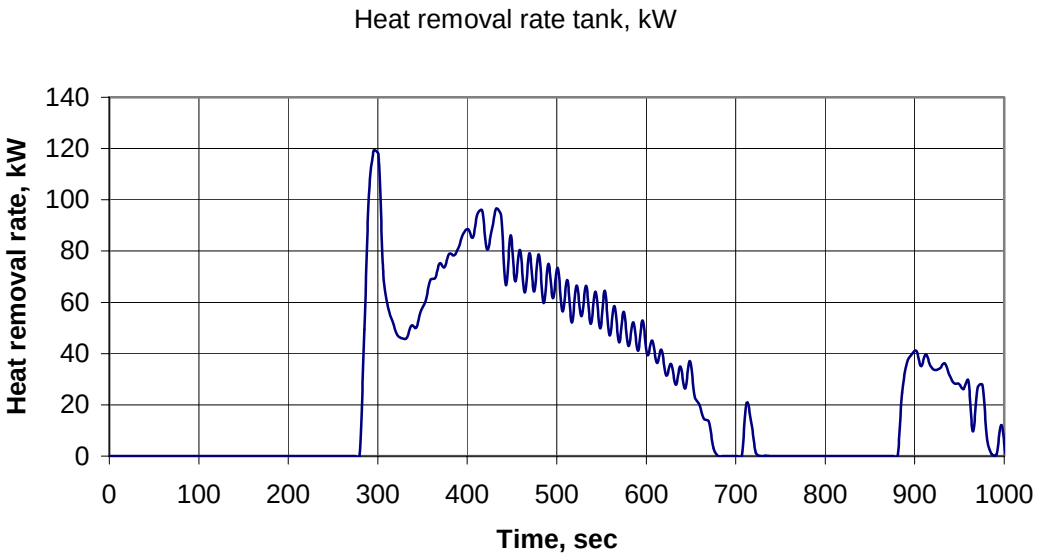

Figure 3.9 Heat removed from tank during the experiment CT-3, Phase I

The steam generation within the tank was close to 0 after t=~700 seconds, because by this time the 5-10cm thick crust had formed on the top of the melt pool (Figure 3.10 shows, that the first 3 layers with thermocouples were quenched by the time t=720 sec). This led to lower heat transfer rates through the crust.

However, after the water flow in the CRGT was stopped at t=880 sec, the water layer above the melt pool in the upper tank began to heat up. The water reached the saturation end the heat removal rate from the tank reached the values of about 40 kW at t=900 sec (Figure 3.9).

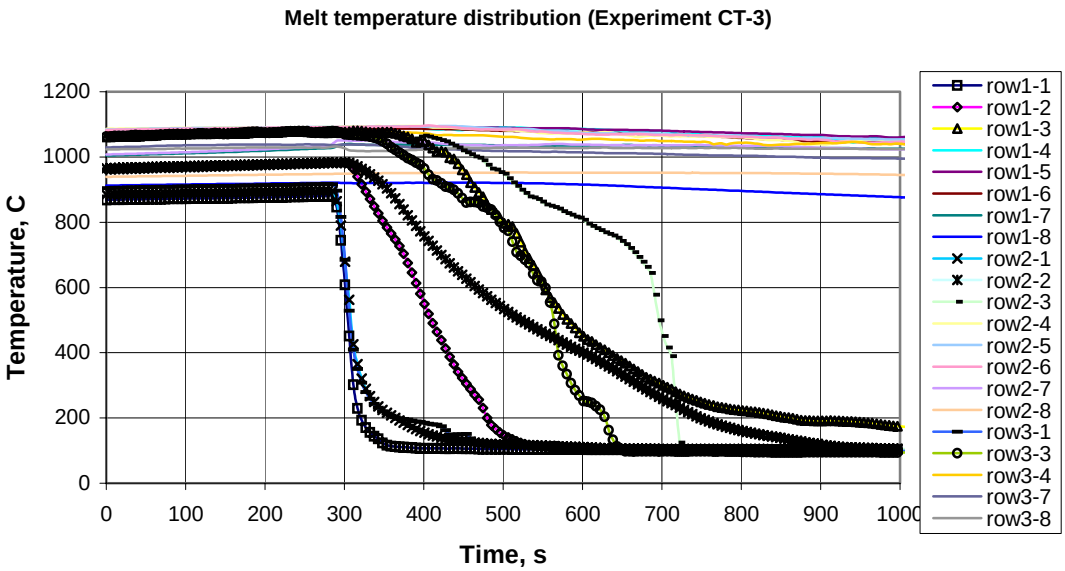

Figure 3.10 Melt temperature distribution during the test CT-3, Phase I

3.4.3.2 PHASE II

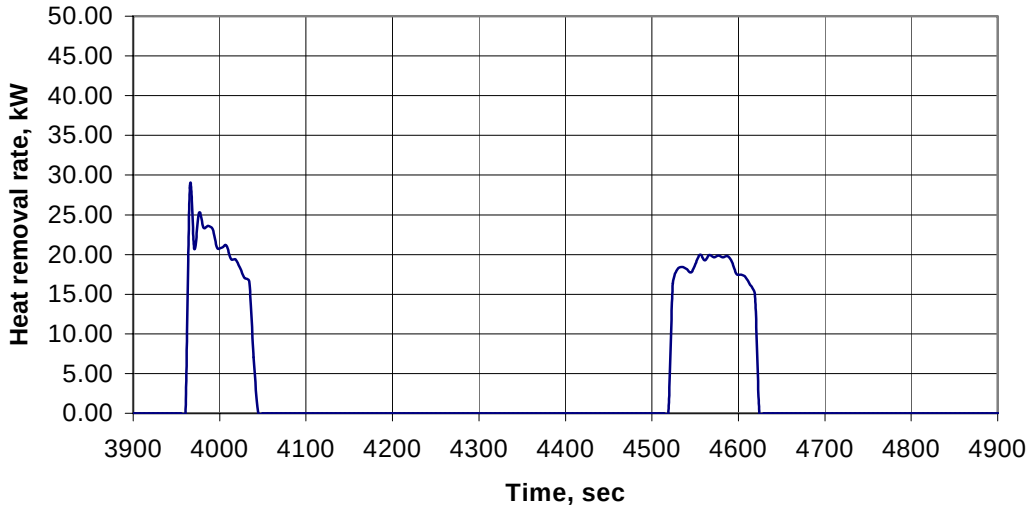

Figure 3.11 Heat removed through CRGT during the experiment CT-3, Phase II

During the time t=880-3980 sec, no additional coolant was supplied to the COMECO test section. The melt pool was reheated to high temperatures, and the second phase of the experiment started. During this phase water at t=12ºC and flow rate of 6.25 g/s was supplied to the CRGT (actual flow rate in the CRGT was fluctuating up to ~9 g/s during the Phase II).

Figure 3.11 shows that the heat removal rate from the CRGT was about 22 kW for the Phase II of the experiment CT-3. The heat removal from the tank was close to 20 kW (Figure 3.12).

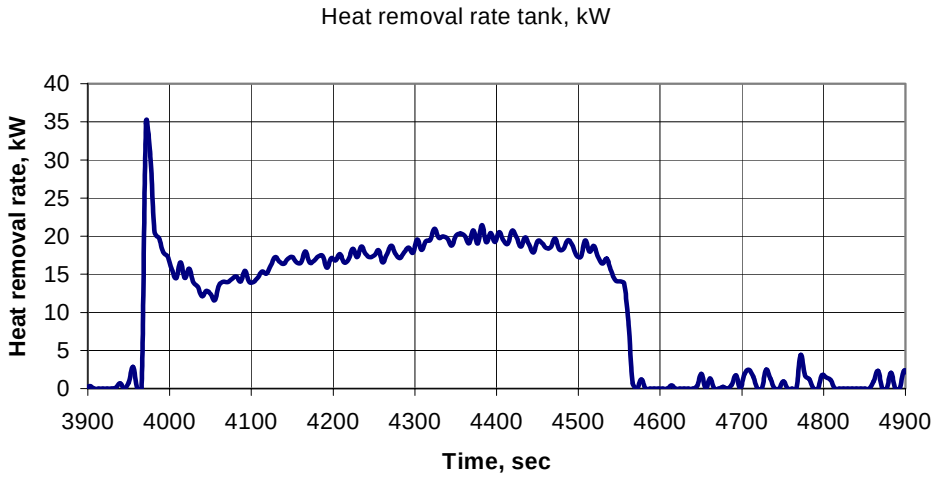

Figure 3.12 Heat removed from tank during the experiment CT-3, Phase II

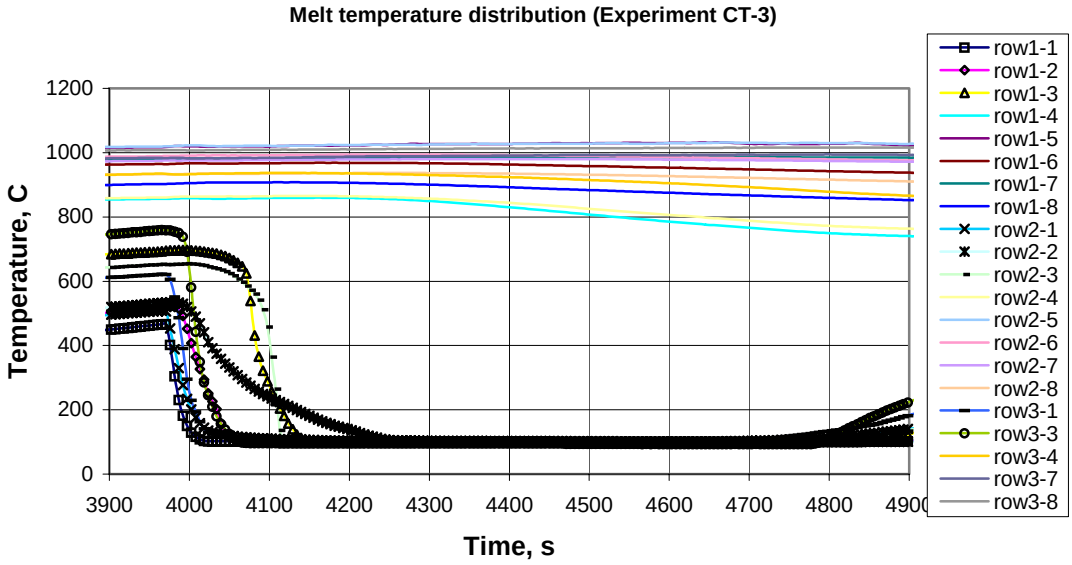

Figure 3.13 Melt temperature distribution during the test CT-3, Phase II

Figure 3.13 present the melt temperature distribution during the Phase II. As it is seen from the Figure, it was not possible to reheat the upper part of the melt to the initial temperatures. However, the tendency observed is similar to the previous phase

of the experiment: the steam flow rate from the tank and, hence, the heat removal rate through the CRGT stabilized after the upper part of the melt pool (5-10 cm) was quenched (at time ~4200 sec).

3.4.3.3 PHASE III

During the time t=4570-7480 sec, no additional coolant was supplied to the COMECO test section. The melt pool was reheated to high temperatures, and the third phase of the experiment started. During this phase water at t=95ºC and flow rate of 62.5 g/s was supplied to the CRGT. The coolant flow in CRGT was stopped at about 8100 seconds.

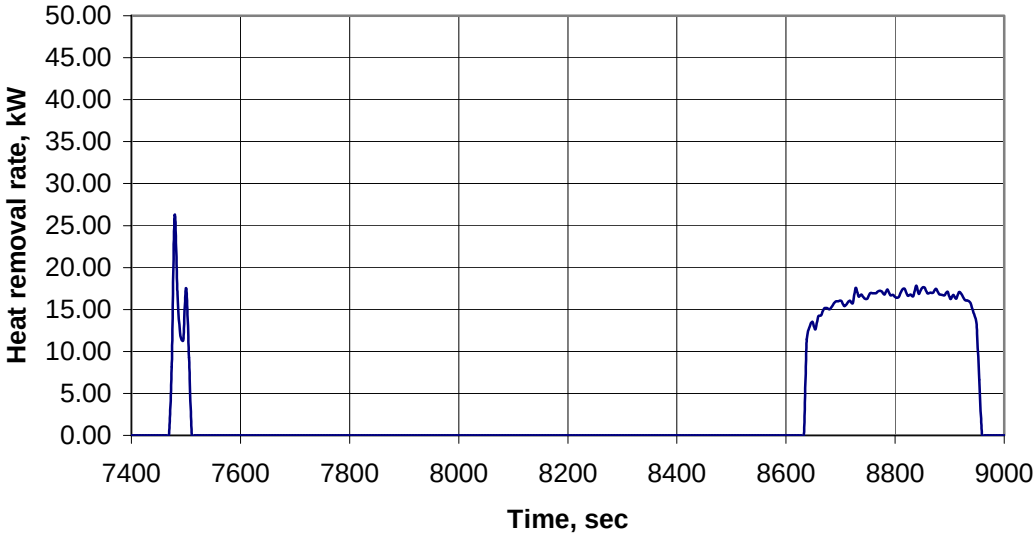

Figure 3.14 Heat removed through CRGT during the experiment CT-3, Phase III

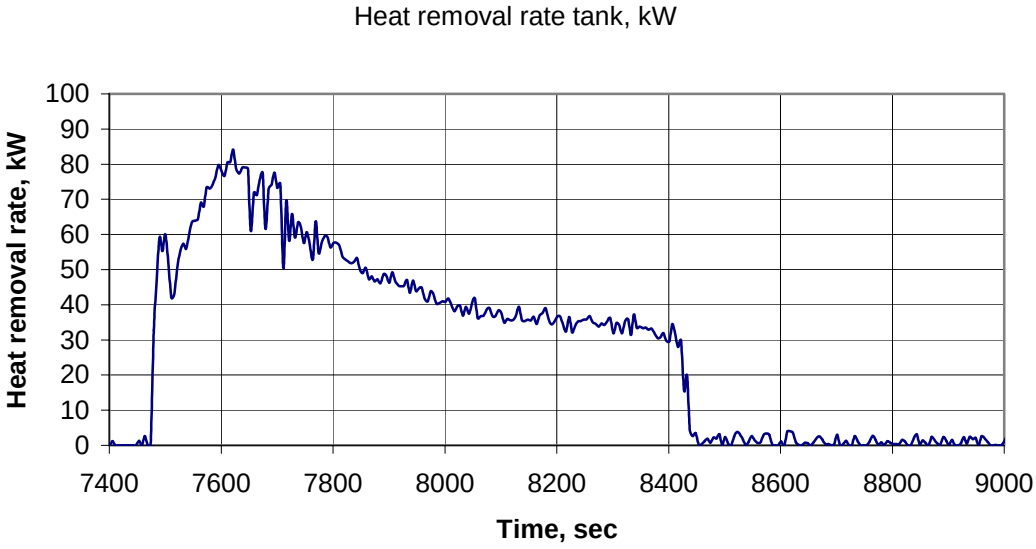

Figure 3.15 Heat removed from tank during experiment CT-3, Phase III

Figures 3.14 and 3.15 present the heat removal rates from the CRGT and tank during the Phase III. As the water temperature in the CRGT was close to the saturation during this Phase, the heat removal from the melt pool did not decrease sharply after the initial peak during the first seconds. This is due to the fact, that for this Phase a rapid reheat of the coolant in the tank to saturation prevented from a time delay, within which the steam generation rates are low (warming up of the coolant in the tank). The average amount of heat removed through the CRGT was about 18 kW.

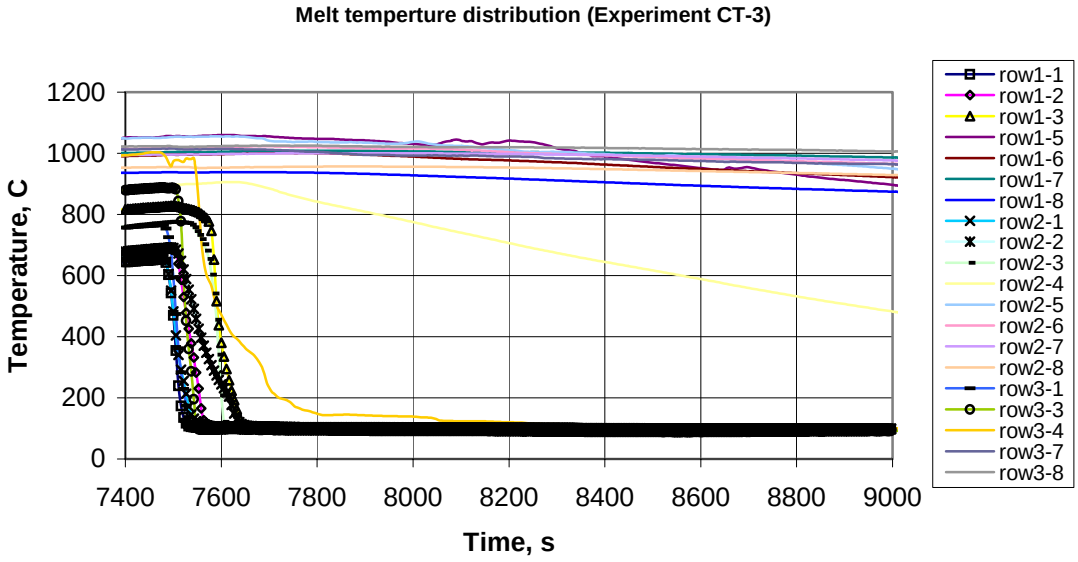

Figure 3.16 Melt temperature distribution during the test CT-3, Phase III

Figure 3.16 presents the temperature distribution in the melt pool during the Phase III. As it is seen from the Figure, during this Phase a partial quenching also at the thermocouple layer 4 (10-15 cm from the top of the melt pool) was achieved.

3.4.3.4 PHASES IV AND V

During the final two phases of the experiment CT-3, the coolant at temperature of 95°C and flow rate of 6.25 g/s (up to ~9 g/s) was supplied through the CRGT. During the Phase V also the additional coolant (at temperature of 95°C) was supplied to the upper tank of COMECO test facility, on top of the melt pool. Quenching experiment was carried out.

The Phase IV started at t=12880 sec, after the reheat of the melt pool. Phase V had started at t=13480 seconds.

During the Phase IV (Figures 3.17 and 3.18) the heat removal rate through the CRGT was 15-20 kW. Lower heat removal rate through the CRGT was registered during the Phase V (top flooding of the melt pool). The stabilized heat removal rate from the tank was close to 50 kW, with a peak of 140 kW at the first moments after the additional water was supplied into the upper tank. During this experiment, similar to the test CT-1, a peak value of the heat transfer coefficient is noted at the beginning of the process. Afterwards, the heat transfer rate drops significantly as crust is formed

on the top of the melt pool. Initial peak is because of the direct contact heat transfer between malt and water.

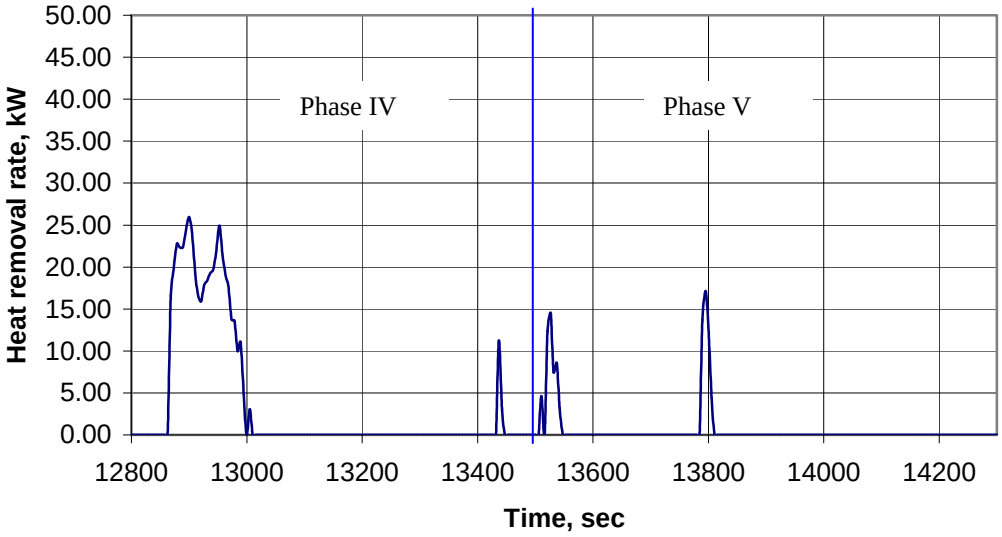

Figure 3.17 Heat removed through CRGT during the experiment CT-3, Phases IV-V

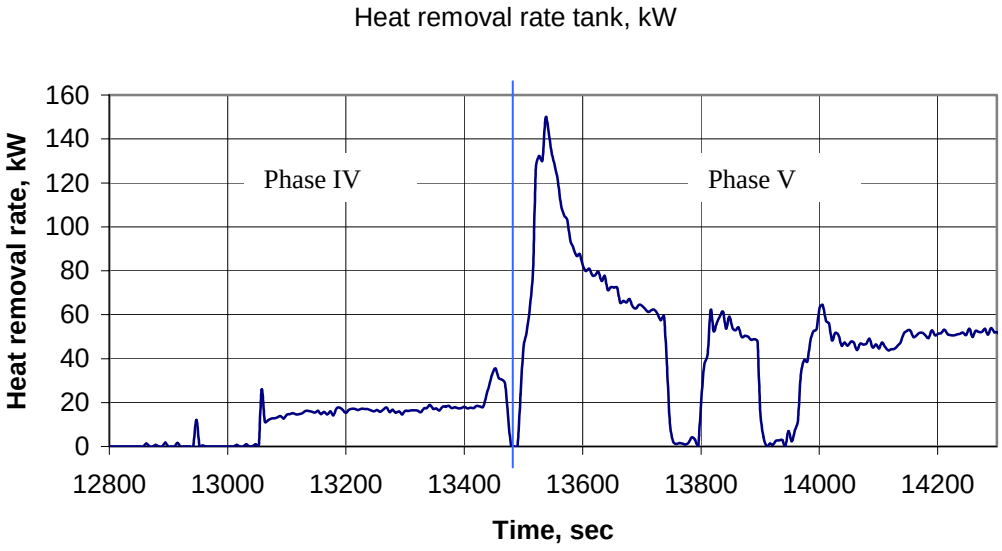

Figure 3.18 Heat removed from tank during experiment CT-3, Phases IV-V

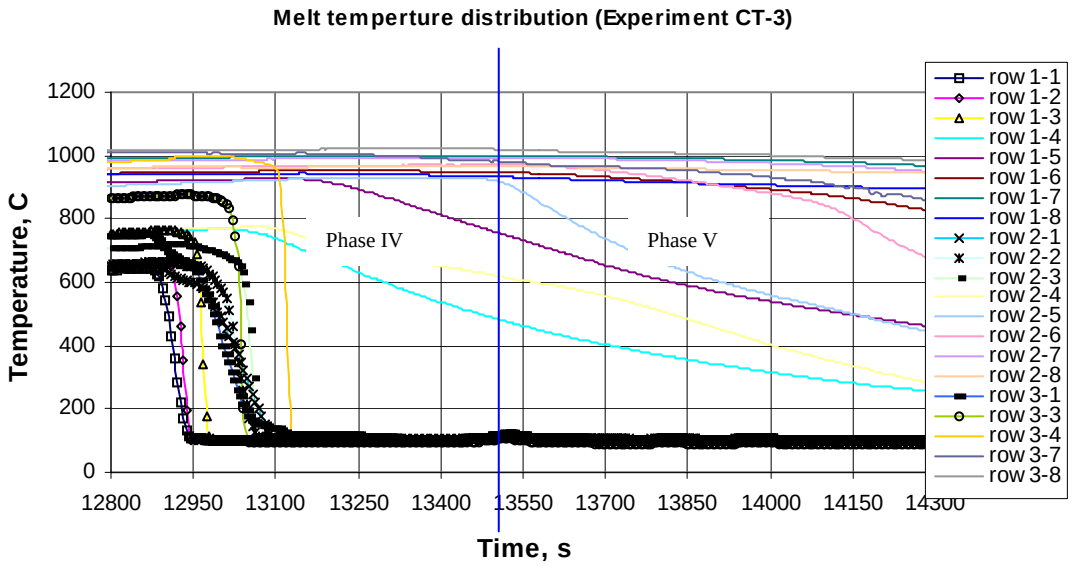

Figure 3.19 Melt temperature distribution during test CT-3, Phases IV-V

The experiment CT-2 is summarized in the Table 3.5.

Table 3.5 Summary of the experiment CT-3

Phase	Flow rate in CRGT, g/s	T_{water} in CRGT, °C	Top flooding	Heat removed through CRGT, kW	Heat removed by top quenching, kW	Total amount of heat removed, kW	Average heat transfer coefficient at CRGT wall , kW/m²
I	62.5	12	NO	38	120-40	158-78	806
II	6.25	12	NO	22	20	40	467
III	62.5	95	NO	15	80-30	95-45	318
IV	6.25	95	NO	25	18	43	531
V	6.25	95	YES	18	150-50	168-68	382

From the results of this experiment it can be concluded, that the maximum heat removal rate from the test section could be up to 170 kW (at the early phases of the top quenching process). After the crust at the top of the melt pool is formed, about 20 kW of heat were removed through the CRGT from the test section by flow through the CRGT and additional 40-50 kW by the top quenching (heat transfer through the crust). The maximum heat removal capacity of the CRGT was 25 kW.

3.5 Analysis

3.5.1 Heat balance

In order to evaluate the experimental heat removal values, the energy conservation requirement for a control volume was applied for the test section. The general form of the energy conservation equation over the time interval Δt is:

$$E_{in}+E_{st}=E_{out}$$

Here E_{in} is the energy supplied to the test section with its heaters, E_{out} is the energy removed from the test section, E_{st} is the energy stored within the control volume.

Heat losses to the environment were not taken into account.

Energy, stored within the test section comprises of:

E_{st}=freezing (phase change) + cooling down of the melt= $-(m\cdot c_{p,m}\cdot\Delta T_m+m\cdot H_{fus})$

Here m is the associated mass of the melt, $C_{p,m}$ is the specific heat of the melt, ΔT_m is the change in melt temperature, H_{fus} is the melt latent heat of fusion.

From the experimental data, the stored heat release rate could be obtained using the formula:

$$\Sigma(\rho_m V_i c_{p,m}(\overline{T}_{t+1}-\overline{T}_t)+m_{pc}H_{fus})/\Delta t$$

where V_i is the melt volume associated with the thermocouple layer, T_{t+1} and T_t are the average melt pool temperatures in the thermocouple layer at recent and previous measurements, Δt is the time interval between the two measurements.

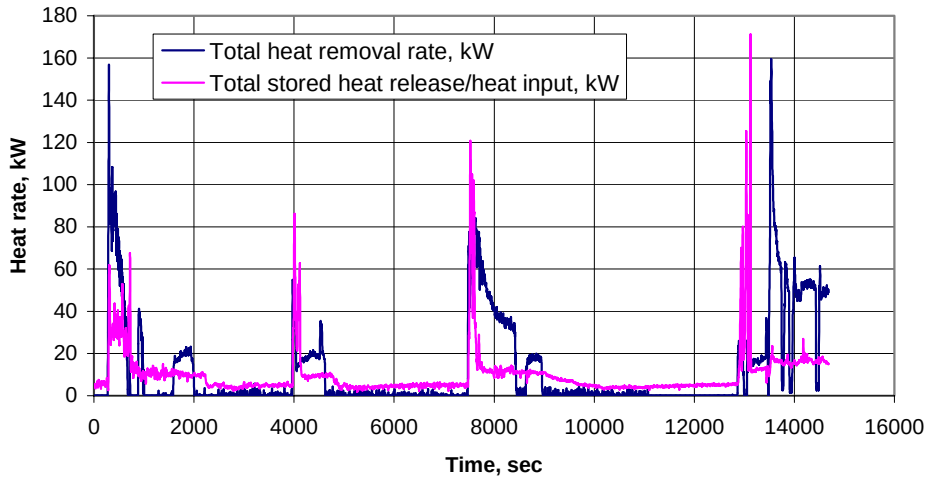

Figure 3.20 Comparison heat removal and stored heat release/heat input rates for the experiment CT-3.

The above formula was applied to estimate the balance between heat removal/heat addition and stored heat rates for the experiment CT-3 data. Figure 3.20 shows the calculation results. As it is seen from this Figure, the higher heat removal rates were encountered during the experiment, which led to the decrease of the melt pool temperature.

The overall heat balance could be evaluated also as a comparison of the cumulative amount of heat (Figure 3.21).

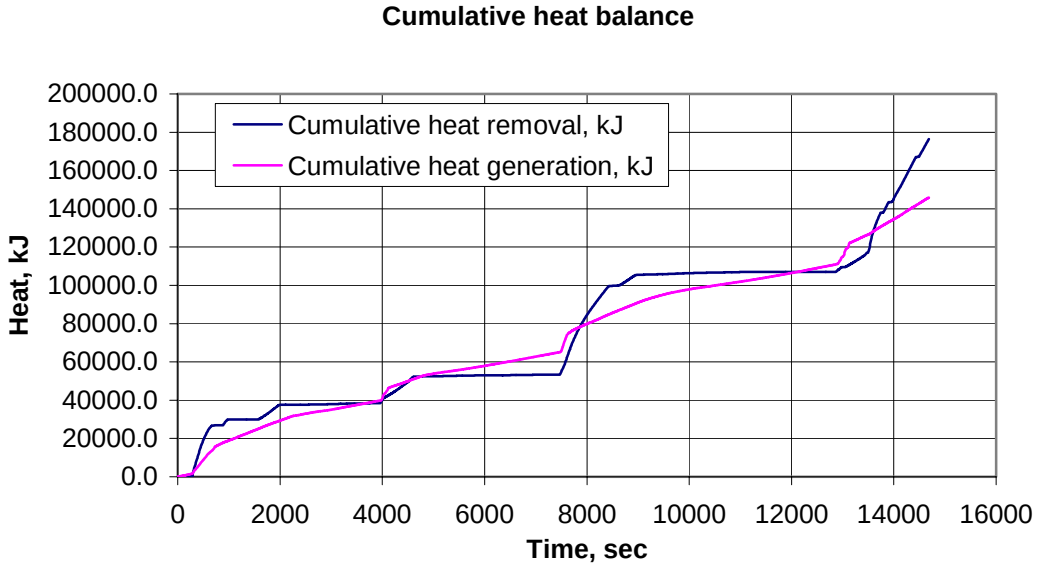

Figure 3.21 Cumulative amount of heat generated and removed during the experiment CT-3.

A zero-dimensional integral analysis has been performed based on consideration of a balance between the heat content inside the melt and heat removal from the melt pool. The basic assumption is that the heat is taken out from the outside surface (in the case of the top flooding of the melt pool) in two ways: film boiling and radiation heat transfer. The following relation for the cooling time can be written:

$$\Delta t = \frac{\rho_m V_m (C_{p,m} \Delta T_m + H_{fus,m}) + W \Delta t}{G_w (H_{wv} + C_{p,w} (T_{sat} - T_w)) + q_{out} S}$$

where Δt is the cooling down time, ρ_m is the melt density, V_m is the melt bed specific volume, W is the power supply, G_w is the water mass flow rate through the CRGT, $H_{w,v}$ is the heat of vaporization of water, q_{out} is the heat removal flux and S is the crust-water interacting area. The numerator in the ratio is responsible for the total heat, which should be removed in order to solidify the bed, and the lower term shows the cooling rate. The equation could be rewritten as:

$$\Delta t = \frac{\rho_m V_m (C_{p,m} \Delta T_m + H_{fus,m})}{(G_w (H_{wv} + C_{p,w} (T_{sat} - T_w)) + q_{out} S) - W}$$

As only partial quenching of the melt pool was reached during the experiment, the equation above was applied to estimate the partial quenching times for the first four phases of the experiment CT-3. The calculation results are presented in the Table 3.6.

Table 3.6 Comparison of experimental and calculated quenching times for the experiment CT-3

Phase	Experimental partial quench time, sec	Calculated quench time, sec
I	438	397
II	180	240
III	160	110
IV	220	314

As it is seen from the Table 3.6, there are some discrepancies between the calculated and experimental quenching times. Longer calculated quenching times for the Phases II and IV were obtained.

3.5.2 Distance, where water becomes saturated

The distance, which liquid has to travel through the CRGT, before it becomes saturated, could be estimated from the formula:

$$l_s = \frac{j_w \rho_w dc_{p,w}(T_s - T_w)}{4q''}$$

For the data from the COMECO experiments, the saturation distance was calculated and the results are presented in the Table 3.8.

Table 3.8 Saturation distance for the water in the CRGT various COMECO tests

Experiment	Flow rate in CRGT, g/s	Subcooling at inlet, °C	Heat removal rate from CRGT, kW	Heat flux through CRGT wall, q", kW/m^2	l_s, cm
CT1-1	62.5	89	18	382	27.7
CT1-2	6.25	89	11	233	7.2
CT1-3	6.25	5	10	212	1
CT3-1	62.5	88	38	806	20.3
CT3-2	6.25	88	22	467	4
CT3-3	62.5	5	15	318	3
CT3-4	6.25	5	25	531	< 1
CT3-5	6.25	5	18	382	< 1

3.6 Conclusions

Three experiments with the molten pool and CRGT model on the COMECO facility were carried out. Each experiment consisted of several phases, during which

the temperature and flow rate of the water inlet to the CRGT were varied. The experiments were performed with open and closed bypass holes at the upper part of the CRGT.

Quenching experiments were carried out. Full quench of the 30 cm deep melt pool was not achieved during the experiments. The thickness of the permeable crust on the top of the molten pool was 5-15 cm. The experimental results show that an average of about 20 kW of additional heat can be removed from the test section through a CRGT surrounded by a melt pool, however, with a crust formed on the surface of the CRGT; which corresponds to a heat removal flux of ~ 350 kW/m^2 for the 30 cm heated height of the CRGT. We believe that with the surface area offered by all the CRGT's in the bottom head of a BWR, it may be possible to remove much of the decay heat generated in a corium melt pool, deposited in the lower head of a BWR.

4. REFERENCES

[1] FARO/TERMOS corium melt quenching experiments”**,** Nuclear Engineering and Design, Volume 189, Issues 1-3, (1999), p. 223-238
[2]I. Lindholm, "A Review on Dryout Heat Fluxes and Coolability of Particle Beds", VTT Research Report, ENE 4/29/2000.
[3] R.J. Lipinski, "A Model for Boiling and Dryout in Particle Beds", Sandia Labs, SAND 82-9765, NUREG/CR-2646, 1982.
[4] R.J. Lipinski, "A Coolability Modal for Post Accident Nuclear Reactor Debris", Nuclear Technology, Vol. 65, pp. 53-66, 1984.
[5] D.H. Cho and L. Bova, "Formation of Dry Pockets During Water Penetration into a Hot Particle Bed", Trans. ANS, Vol. 41, 1983.
[6] T. Ginsberg, J. Klein, J. Klages, C.E. Schwarzand J.C. Chen, "Transient Core Debris Heat Removal Experiments and Analysis", presented at the International Meeting on Thermal Nuclear Reactor Safety, Chicago, Illinois, 1982.
[7] V.X. Tung, V.K. Dhir and D. Squarer, "Quenching by Top Flooding of a Heat Generating Particulate Bed With Gas Injection at the Bottom", Proc. of the 6th Information Exchange Meeting on Debris Coolability, 1986.
[8] M. Kaviany, "Principles of heat transfer in porous media", Second Edition, Springer, 1995.
[9] M.J. Konovalikhin, Z.L. Yang, M. Amjad and B.R. Sehgal,"On Dryout Heat Flux of s Particle Debris Bed with a Downcomer", ICONE-8, Baltimore, USA, April, 2000.
[10] M.J. Konovalikhin and B.R Sehgal, "Investigation of Volumetrically Heated Debris Bed Quenching", ICONE-9, Nice, France, April 8-12, 2001.
[11] H.S. Carslaw and J.C. Jaeger, "Conduction of Heat in Solids", Second edition, Oxford University Press, London, 1962,
[12] J.V. Beck, B. Blacwell, Ch. Clair, "Inverse Heat Conduction III-Posed Problems", Walay-Interscience, 1985.
[13] Stolyarova, V.L:, Green, J., *Physico-chemical properties of the Cao-B_2O_3 system*, NPS-EDPR-97-22 Report (1997).

www.ski.se

STATENS KÄRNKRAFTINSPEKTION
Swedish Nuclear Power Inspectorate

POST/POSTAL ADDRESS SE-106 58 Stockholm
BESÖK/OFFICE Klarabergsviadukten 90
TELEFON/TELEPHONE +46 (0)8 698 84 00
TELEFAX +46 (0)8 661 90 86
E-POST/E-MAIL ski@ski.se
WEBBPLATS/WEB SITE www.ski.se